Entanglement in an open Heisenberg Spin Chain

Submitted in partial fulfilment of the requirement for the degree of

Master in Mathematics

Department of Mathematics and Statistics,

Memorial University at Newfoundland

Submitted By
Subhendu Paul

September 2018

ABSTRACT

We analyze the time evolution of a spin chain of three qubits with nearest-neighbour Heisenberg XX interaction, coupled to two thermal reservoirs. We use the 'reduced density matrix approach' to calculate the populations and correlations (concurrence) among the spins. The spin-reservoir interaction is of the energy conserving type. This allows us to analyze the evolution analytically without approximations – yielding explicit, yet complicated formulas for the spin dynamics. To analyze the latter and discuss it as a function of the various physical parameters and time (intial conditions, termperatures, coupling strenghts), we resort to numerical methods.

Our main finding is that the external noise (coupling to reservoirs) causes the appearence of an asymptotic, stationary (time-periodic) regime for the dynamics of concurrence. We discuss the dependence of the relaxation time and the characteristics of the regime itself, on the various parameters.

ACKNOWLEDGEMENT

First and foremost, I would like to thank my family members for their continuing and boundless support and encouragement throughout my education. I would like to thank my supervisor Prof. Marco Merkli whose guidance and advice has proven invaluable to my study and research work. I am greatly indebted to him for the academic opportunities has has provided me. I would also like to mention Dr. Alex Bihlo and thank him for his help in my learning of numerical methods and developing MATLAB codes. I would like to thank the department of mathematics and statistic at Memorial University for the opportunity to study here. I also owe a lot to the professors I have had entire the master period. To name a few I would like to thank Dr. Deping Ye, Dr. Yuan Yuan and the many others who have had a profound and positive effect on my learning. In addition, I would like to thank the administrative stuff at the department for their help with all of the logistic that come with being a student; they have made my time here infinitely easier and very enjoyable. My friend Dr. Alireza encouraged me a lot to finish the project work with significant outcomes. Finally, I thank my wife Deepali Chatterjee for her constant support throughout the completion of my degree. By necessity, a list of acknowledgements omits many to whom thanks are due; there are many other friends, colleagues and professors who have helped me but not listed here and I give them my thanks as well.

Contents

1. Introduction

1.1 Overview

Quantum computers, expected to be significantly faster than classical (present) ones, are based on entanglement [**1**, **2**], a quantum-mechanical phenomenon allowing to implement quantum data buses which will transport a required quantum state with high accuracy. Several techniques have been introduced to develop quantum data buses; some of which are involving spin (or, quibit) chains, which have drawn significant attention [**3-11**]. The crucial property of entanglement is very much affected by noise. However, it is quite impossible to consider an isolated quantum system; there is always some coupling to (interaction with) the surrounding environment, which influences entanglement adversely. To understand the environmental effect, we can model the environment as a bosonic heat reservoir in a thermal equilibrium state (say, at room temperature or a cooled-down environment) [**12-15**], or in a non-equilibrium 'thermal' state [**16**, **17**] (in presence of a temperature gradient). In both cases, equilibrium and non-equilibrium, the temperature of the reservoirs (for equilibrium) and the temperature difference between reservoirs (for non-equilibrium) directly affect the entanglement of the quantum system [**18**, **19**].

Apart from the spin-reservoir coupling for a spin chain and reservoir system, the spin-spin interaction is also crucial, and we merely consider the coupling between two consecutive spins. In this context, a myriad works have been reported to consider various Heisenberg interactions, see for instance Ref. [**20**] and references there in.

Many studies use an approximation, the Lindblad–Markovian master equation to describe the spin chain and bosonic reservoirs [**21**]. Besides the master equation, the approach of 'reduced density matrix' has been used to investigate reservoir effect on entanglement for equilibrium and non-equilibrium cases [**22-27**]. In those work, researchers focused on bipartite entanglement between two qubits (=spins) from the chain in contact with the reservoir.

In this thesis, we consider a linear spin chain of three spins connected to two bosonic reservoirs. Here we consider the 'Heisenberg XX' interaction between consecutive spins. We first calculate the density matrix for the three spins, taking the trace over the two reservoirs. The diagonal elements of the density matrix represent the populations (probabilities of occupation) of the states. Applying the procedure of the 'reduced density matrix', we obtain the joint density matrix of spins 1 and

2 (and that of spins 1 and 3), then for spin 1 alone and for spin 2 alone. We study the present system in three different cases: without reservoir coupling, with coupling to a single reservoir, and with coupling to two reservoirs. Our goal is to investigate the effect of a single reservoir as well as double reservoirs on the concurrences (= measure of entanglement). The concurrence as well as the populations of the system depend significantly on the initial state. We study three kinds of entanglement: bipartite entanglement, the concurrence for tripartite systems, and intrinsic three spin entanglement. We consider four different initial states for the system and vary the values of the reservoir coupling constant and temperature.

The thesis is organized as follows. In chapter 2 we describe our model along with the analytical expression of the density matrices and concurrences. The numerical calculations and results are reported in chapter 3 with discussion. Finally, we give a conclusion in chapter 4.

1.2 Quick Outline of our Main Results

In this thesis, we consider a linear chain of three interacting spins coupled to a bosonic field. The spins are often referred to as the *system*, the fields as the *reservoir(s)*. In the initial states we analyze, each spin and each reservoir is always uncorrelated with all others (more precisely, we take initial product states, or, disentangled states). All initial reservoir states are thermal equilibria. The interaction among the spins is governed by the ubiquitous Heisenberg XX Hamiltonian. The coupling to the reservoirs is energy-conserving, which is physically relevant and describes situations where the total energy of each subsystem is constant, but important correlations (entanglement) among the parts are still built up.

We focus on three interesting cases:

- *Case I*: System without reservoir coupling (as indicated in Figure 1.1, left)
- *Case II*: System with coupling to a single reservoir (as indicated in Figure 1.1, middle)
- *Case III*: System with coupling to two reservoirs (as indicated in Figure 1.1, right)

We analyze the system dynamics (the spin dynamics) for different spin initial states, for different system-reservoir coupling strenghts, as well as for different reservoir temperatures.

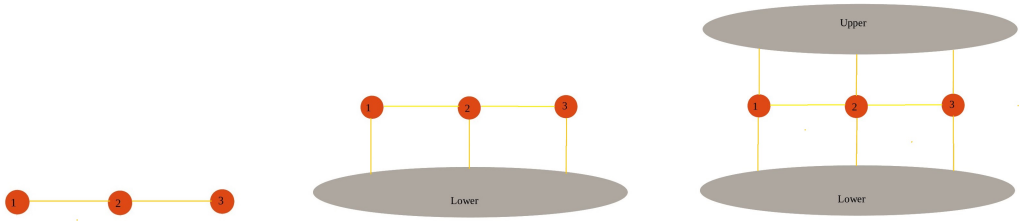

Figure 1.1: The three cases: spins just interacting with each other, and interacting additionally with one or two reservoirs.

The **main results** of the thesis are given below:

- *Case I*: We take four different initial states (all disentangled, i.e., having zero concurrence) and calculate the spin populations and concurrences as a function of time. As there is no coupling to reservoirs (external noise), the system dynamics is periodic in time. We identify initial spin states for which the Heisenberg XX interaction produces maximum entanglement between two spins. There are also initial states for which entanglement is *never* (at no time) created. Generally, the amount of concurrence created significantly depends on initial state.

- *Case II*: We take a specific initial spin state and vary the values of the reservoir temperature and of the coupling constant. We find that the effect of the coupling to the external noise (reservoir) is twofold:
  (i) There appears a *transient time regime* for relatively small times, during which the system dynamics is complicated. Then, after a certain characteristic time, the dynamics settles into a periodic asymptotic regime. The relaxation time (to reach the periodic regime) depends on the system-reservoir coupling strength as well as on the reservoir temperature. We find that the relaxation time increases if either of the temperature or the coupling is decreased. (This is of course physically reasonable, as a stronger coupling amounts to a stronger reservoir effect.)
  (ii) The amplitude of oscillation in the concurrence (correlations) is *reduced* compared to the case I. The stronger the coupling constant or the higher the temperature, the smaller this amplitude. So the generic effect here on the system correlation is to reduce the amount of temporal variation in the concurrence.

  We also show that the two-spin entanglement of nearest neighbour spins is *stronger* than that of two spins apart.
- *Case III*: We consider the system-reservoir coupling constants for reservoirs 1 and 2 to be the same. Then, if both reservoirs are at the same temperature, the present case reduces to that of a single one (at the common temperature and coupling constant). However, when there is a *temperature difference*, then we are now in a *non-equilibrium situation*. As in the single-reservoir situation (case II), there is a stationary regime for the concurrence, which is reached after a characteristic time. Let T and $T+\Delta T \geq T$ be the temperatures of the two reservoirs. We show that the relaxation time increases if T decreases, and it increases as well when ΔT shrinks. We conclude that the more we are in a non-equilibrium situation (ΔT large), the quicker the stationary regime is reached.

1.3 Density Matrix, Pure and Mixed states

The density matrix represents quantum states (or an ensemble of quantum states) [**21**, **29**]. A pure state can be described by a normalized vector $|\psi(t)\rangle$ (the 'wave function') in Hilbert space, $\mathbb{C}^2$ for a single qubit (spin). The associated density matrix $\rho(t)$ is defined as the outer product

$$\rho(t) = |\Psi(t)\rangle\langle\Psi(t)|. \tag{1.1}$$

In case of pure state $\rho^2 = \rho$ so ρ is a projector. If we consider a particular state $|\phi(t)\rangle$, the integral $\langle\phi(t)|\rho(t)|\phi(t)\rangle$ gives the probability of finding a particle in the state $|\phi(t)\rangle$.
A mixed state is determined by a set $\{p_i, |\psi_i\rangle\}$, where the $|\psi_i\rangle$ are pure states and the p_i are probabilities. It is given by the density matrix

$$\rho = \sum_i p_i |\psi_i\rangle\langle\psi_i| \tag{1.2}$$

We have $0 \leq p_i \leq 1$ and $\sum_i p_i = 1$. A mixed state is always described by a density matrix which is not a projector, i.e., which satisfies $\mathrm{Tr}(\rho^2) < 1$ (see also below).

Properties of the density matrix:

1)	ρ is Hermitian	$\rho^\dagger = \rho$
2)	Normalization	$\mathrm{Tr}(\rho) = 1$
3)	Positivity	$\rho \geq 0$
4)	Purity	$\mathrm{Tr}(\rho^2)$ $\begin{cases} = 1 \text{ if } \rho \text{ is pure} \\ < 1 \text{ if } \rho \text{ is mixed} \end{cases}$

Here, Tr denotes the trace. Note, if a matrix ρ satisfies 1) – 3) and $\mathrm{Tr}(\rho^2) = 1$, then ρ is a rank-one projection. So a pure state is always given by a rank-one projection density matrix.

■ **Example 1.1**

$$|\psi_1\rangle = \frac{1}{\sqrt{2}}(|0\rangle + |1\rangle) \tag{1.3}$$

is a pure state where $|0\rangle$ and $|1\rangle$ represent spin down and spin up states, respectively. ■

■ **Example 1.2** The density matrix ρ_1 corresponding the pure state $|\psi_1\rangle$ can be written in the basis $\{|0\rangle, |1\rangle\}$ as

$$\begin{aligned} \rho_1 &= |\psi_1\rangle\langle\psi_1| \\ &= \frac{1}{2}\Big[|0\rangle\langle 0| + |0\rangle\langle 1| + |1\rangle\langle 0| + |1\rangle\langle 1|\Big] \end{aligned} \tag{1.4}$$

Now,

$$|0\rangle\langle 0| = \begin{pmatrix} 0 \\ 1 \end{pmatrix}(0 \;\; 1) = \begin{pmatrix} 0 & 0 \\ 0 & 1 \end{pmatrix}, \tag{1.5}$$

$$|0\rangle\langle 1| = \begin{pmatrix} 0 \\ 1 \end{pmatrix}(1 \;\; 0) = \begin{pmatrix} 0 & 0 \\ 1 & 0 \end{pmatrix}, \tag{1.6}$$

$$|1\rangle\langle 0| = \begin{pmatrix} 1 \\ 0 \end{pmatrix}(0 \;\; 1) = \begin{pmatrix} 0 & 1 \\ 0 & 0 \end{pmatrix} \tag{1.7}$$

and

$$|1\rangle\langle 1| = \begin{pmatrix} 1 \\ 0 \end{pmatrix}(1 \;\; 0) = \begin{pmatrix} 1 & 0 \\ 0 & 0 \end{pmatrix}. \tag{1.8}$$

Combining (1.4), (1.5), (1.6), (1.7) and (1.8), we get

$$\rho_1 = \frac{1}{2}\begin{pmatrix} 1 & 1 \\ 1 & 1 \end{pmatrix}. \tag{1.9}$$

It is clear from (1.9) that

$$\mathrm{Tr}(\rho_1) = 1,$$

and

$$\mathrm{Tr}(\rho_1^2) = \mathrm{Tr}\Big(\frac{1}{4}\begin{pmatrix} 1 & 1 \\ 1 & 1 \end{pmatrix}\begin{pmatrix} 1 & 1 \\ 1 & 1 \end{pmatrix}\Big) = 1$$

■

■ **Example 1.3** Consider the mixed state obtained by taking the state $|1\rangle$ with probability 1/2 and the state $|\psi_1\rangle$, defined in (2.70), with probability 1/2. Using the expression (1.2) the mixed state can be represented as a matrix ρ_2 in the basis $\{|0\rangle, |1\rangle\}$:

$$\rho_2 = \frac{1}{2}|1\rangle\langle 1| + \frac{1}{2}|\psi_1\rangle\langle\psi_1| \tag{1.10}$$

It follows from (1.8) and (1.4)

$$\begin{aligned} \rho_2 &= \frac{1}{2}\begin{pmatrix} 1 & 0 \\ 0 & 0 \end{pmatrix} + \frac{1}{4}\begin{pmatrix} 1 & 1 \\ 1 & 1 \end{pmatrix} \\ &= \frac{1}{4}\begin{pmatrix} 3 & 1 \\ 1 & 1 \end{pmatrix} \end{aligned} \tag{1.11}$$

We can easily see that

$$\mathrm{Tr}(\rho_2) = 1$$

and

$$\mathrm{Tr}(\rho_1^2) = \mathrm{Tr}\Big(\frac{1}{16}\begin{pmatrix} 3 & 1 \\ 1 & 1 \end{pmatrix}\begin{pmatrix} 3 & 1 \\ 1 & 1 \end{pmatrix}\Big) = \frac{3}{4} < 1.$$

■

1.4 Partial Trace

Let $\mathscr{H}_{AB} = \mathscr{H}_A \otimes \mathscr{H}_B$ be the tensor product of two separable Hilbert spaces $\mathscr{H}_A$ and $\mathscr{H}_B$, and set $\rho_{AB} = \rho_A \otimes \rho_B \in \mathscr{B}(\mathscr{H}_{AB})$ where $\rho_A \in \mathscr{B}(\mathscr{H}_A)$ and $\rho_B \in \mathscr{B}(\mathscr{H}_B)$. The partial trace of ρ_{AB} over $\mathscr{H}_B$ is given by

$$\mathrm{Tr}_B(\rho_{AB}) = \rho_A \mathrm{Tr}_{\mathscr{H}_B}(\rho_B) \tag{1.12}$$

Let $\{|a_i\rangle\}$ and $\{|b_i\rangle\}$ be the basis of $\mathscr{H}_A$ and $\mathscr{H}_B$, respectively. We can decompose any density matrix ρ_{AB} on $\mathscr{H}_A \otimes \mathscr{H}_B$ as

$$\rho_{AB} = \sum_{ijkl} C_{ijkl} |a_i\rangle\langle a_j| \otimes |b_k\rangle\langle b_l|, \tag{1.13}$$

and the partial trace of ρ_{AB} over $\mathscr{H}_B$ is given by linearity as

$$\mathrm{Tr}_B(\rho_{AB}) = \sum_{ijkl} C_{ijkl} |a_i\rangle\langle a_j| \langle b_k|b_l\rangle = \sum_{ijk} C_{ijkk} |a_i\rangle\langle a_j|. \tag{1.14}$$

$\mathrm{Tr}_B(\rho_{AB})$ is a density matrix ρ_A on $\mathscr{H}_A$ and $\mathrm{Tr}(|b_k\rangle\langle b_l|) = \langle b_k|b_l\rangle = \delta_{k,l}$ (Kronecker delta).

1.5 Reduced Density Matrix

Suppose the composite, combination of two systems A and B, is in the state ρ_{AB}. The reduced density operator of the system A can be obtained by taking the partial trace over B, and is defined by

$$\rho_A = \mathrm{Tr}_B \rho_{AB}. \tag{1.15}$$

Here, Tr_B is the partial trace over the degrees of freedom of the system B, defined by linear extension of the relation

$$\mathrm{Tr}_B(|a_1\rangle\langle a_2| \otimes |b_1\rangle\langle b_2|) \equiv |a_1\rangle\langle a_2| \mathrm{Tr}(|b_1\rangle\langle b_2|) \tag{1.16}$$

with $|a_1\rangle$, $|a_2\rangle$, $|b_1\rangle$, $|b_2\rangle$ arbitrary vectors in $A(B)$.

■ **Example 1.4** Suppose ρ_{AB} is given by

$$\rho_{AB} = \frac{1}{2}\Big[|01\rangle\langle 01| - |01\rangle\langle 10| - |10\rangle\langle 01| + |10\rangle\langle 10|\Big] \tag{1.17}$$

Taking partial trace according to the definition (1.14), we have

$$\begin{aligned} \mathrm{Tr}_B(\rho_{AB}) &= \frac{1}{2}\Big[|0\rangle\langle 0|\langle 1|1\rangle - |0\rangle\langle 1|\langle 1|0\rangle - |1\rangle\langle 0|\langle 0|1\rangle + |1\rangle\langle 1|\langle 0|0\rangle\Big] \\ &= \frac{1}{2}\Big[|0\rangle\langle 0| + |1\rangle\langle 1|\Big] \\ &= \frac{1}{2}\mathbb{I} \end{aligned} \tag{1.18}$$

The reduced is state $\rho_A = \mathrm{Tr}_B(\rho_{AB}) = \frac{1}{2}\mathbb{I}$. ■

1.6 Heisenberg Model

The Heisenberg model accounts only for the coupling between nearest neighbours of qubits. In three dimension, the interaction Hamiltonian for the Heisenberg model of N qubits is given by

$$H_{int}^{XYZ} = \sum_{j=1}^{N-1} (J_x \sigma_j^x \sigma_{j+1}^x + J_y \sigma_j^y \sigma_{j+1}^y + J_z \sigma_j^z \sigma_{j+1}^z) \tag{1.19}$$

where J_x, J_y and J_z are coupling constants and the Pauli spin matrices are given by

$$\sigma^x = \begin{pmatrix} 0 & 1 \\ 1 & 0 \end{pmatrix}, \quad \sigma^y = \begin{pmatrix} 0 & -i \\ i & 0 \end{pmatrix}, \quad \sigma^z = \begin{pmatrix} 1 & 0 \\ 0 & -1 \end{pmatrix}.$$

In the above equation, σ_j^α ($\alpha = x, y, z$) denotes the Pauli matrix σ^α acting only on the j-th qubit. We obtain the Heisenberg XX Hamiltonian, H_{int}^{XX}, by setting $J_x = J_y$ and $J_z = 0$. This is the simplest model of a quantum spin chain with rotational symmetry. Moreover, in the XX model the magnetization is a conserved quantity. The interaction Hamiltonian H_{int}^{XX} acts upon the tensor product $(\mathbb{C}^2)^{\otimes 3}$ of dimension 2^3. A detailed description of the Heisenberg XX model can be found in [**28**].

1.7 The bosonic field

1.7.1 Tensor products and Fock space

Let $\{\alpha_k\}_{k\geq 1}$ and $\{\beta_l\}_{l\geq 1}$ be two orthonormal bases of two separable Hilbert spaces $\mathscr{H}_A$ and $\mathscr{H}_B$, respectively. The tensor product of $\mathscr{H}_A$ and $\mathscr{H}_B$ is defined as $\mathscr{H}_A \otimes \mathscr{H}_B$ is a separable Hilbert space with basis $\{\alpha_k \otimes \beta_l\}_{k,l\geq 1}$. Any state $\phi \in \mathscr{H}_A \otimes \mathscr{H}_B$ can be expressed as

$$\phi = \sum_{k,l\geq 1} A_{kl} \alpha_k \otimes \beta_l \quad \text{where} \quad A_{kl} = \langle \alpha_k \otimes \beta_l, \phi \rangle \tag{1.20}$$

The bases $\{\alpha_k\}_{k\geq 1}$ and $\{\beta_l\}_{l\geq 1}$ have the following property

$$\langle \alpha_k \otimes \beta_l, \alpha_k' \otimes \beta_l' \rangle = \langle \alpha_k \otimes \alpha_k' \rangle \langle \beta_l \otimes \beta_l' \rangle = \delta_{kk'} \delta_{ll'} \tag{1.21}$$

The finite tensor product is written as

$$\bigotimes_{1\leq j\leq n} \mathscr{H}_j = \mathscr{H}_1 \otimes \mathscr{H}_2 \otimes \ldots \otimes \mathscr{H}_n \tag{1.22}$$

Let $\mathscr{H}$ be a fixed Hilbert space. The symmetric subspace $\mathrm{Sym}(\mathscr{H}^{\otimes^n})$ of $\mathscr{H}^{\otimes^n}$ consists of all vectors $\mathscr{T} \in \mathscr{H}^{\otimes^n}$ such that

$$f_\sigma(\mathscr{T}) = \mathscr{T}, \tag{1.23}$$

where σ is any permutation of $1, 2, \ldots, n$ and, for all $k_1, \ldots, k_n \in \mathscr{H}$,

$$f_\sigma(k_1 \otimes \cdots \otimes k_n) = k_{\sigma(1)} \otimes \cdots \otimes k_{\sigma(n)}. \tag{1.24}$$

(The action of f is extended by linearity.)

The **bosonic Fock space** over (a single-particle Hilbert space) $\mathscr{H}$ is defined as

$$\mathscr{F}(\mathscr{H}) = \bigoplus_{n\geq 0} \mathrm{Sym}(\mathscr{H}^{\otimes^n}), \tag{1.25}$$

where $\mathscr{H}^{\otimes n} = \mathscr{H} \otimes \cdots \otimes \mathscr{H}$ (n factors) and by definition, $\mathscr{H}^{\otimes 0} = \mathbb{C}$.

1.7.2 Thermal quantum fields

The reservoir R, a very large quantum system, is in thermal equilibrium state at temperature $T = 1/\beta$ where β is the inverse temperature. Generally, a reservoir is a quantum gas, bosonic or fermionic, with a given radiation field or particle density. The reservoirs we consider in the present model are spatially infinitely extended gases of Bosons with dispersion relation $\omega(k) = |k|$. We consider Bose gas in a phase without any condensate. We derive the state of the reservoir by using a thermodynamic limit of finite-volume equilibrium states with fixed density and temperature. The Hilbert space for corresponding the reservoir R, the so-called Araki–Woods representation [**30**, **31**], is given by

$$\mathscr{H}_R = \mathscr{F}(L^2(\mathbb{R}^3, d^3k)) \otimes \mathscr{F}(L^2(\mathbb{R}^3, d^3k)), \tag{1.26}$$

where $L^2(\mathbb{R}^3, d^3k)$ is the space of square-integrable complex-valued functions in momentum representation, and $\mathscr{F} \equiv \mathscr{F}(L^2(\mathbb{R}^3, d^3k))$ is the bosonic Fock space over the single particle wave function space $L^2(\mathbb{R}^3, d^3k)$.

A general element in $\mathscr{F}$ is a sequence $\psi = (\psi_0, \psi_1, \psi_2, \ldots)$ with $\psi_i \in \mathrm{Sym}\big(L^2(\mathbb{R}^3, d^3k)\big)^{\otimes i}$ for $i > 0$ (and $\psi_0 \in \mathbb{C}$), satisfying

$$||\psi||^2 = \sum_{i \geq 0} ||\psi_i||^2_{L^2(\mathbb{R}^{3i}, d^{3i}k)} < \infty. \tag{1.27}$$

The equation (1.27) represents the norm of the bosonic Fock space. Now we define, for any $f \in L^2(\mathbb{R}^3, d^3k)$, the *annihilation operator* $a(f)$ and *creation operator* $a^*(f)$, the adjoint of $a(f)$, on Fock space $\mathscr{F}$.

The *creation operator* $a^*(f)$ maps the n-sector into $(n+1)$-sector and acts on a n-particle sector, for $\psi = (0, \ldots, \psi_n, 0, \ldots)$, as

$$(a^*(f)\psi)_k = \begin{cases} 0 & \text{if} \quad k \neq n+1 \\ \sqrt{n+1}\, \mathsf{S} f \otimes \psi_n & \text{if} \quad k = n+1. \end{cases} \tag{1.28}$$

The symmetrization operator S is defined as

$$(\mathsf{S} f \otimes \psi_n)(k_1, \ldots, k_{n+1}) = \frac{1}{(n+1)!} \sum_{j=1}^{n+1} f(k_j) \psi_n(k_1, \ldots, k_{j-1}, k_{j+1}, \ldots, k_{n+1}).$$

The *annihilation operator* $a(f)$ maps the n-sector into the $(n-1)$-sector. The operator acts on a n-particle sector, for $\psi = (0, \ldots, \psi_n, 0, \ldots)$, as

$$(a(f)\psi)_k = \begin{cases} 0 & \text{if} \quad k \neq n-1 \\ \sqrt{n} \int_{\mathbb{R}^3} \bar{f}(k_n) \psi_n(k_1, \ldots, k_n) d^3k_n & \text{if} \quad k = n-1. \end{cases} \tag{1.29}$$

The bosonic field operator is the self-adjoint operator defined as

$$\phi(f) = \frac{1}{\sqrt{2}}(a(f) + a^*(f)). \tag{1.30}$$

In general, we define bosonic creation and annihilation operators as $a^*(k)$ and $a(k)$ for $k \in \mathbb{R}^3$, respectively, which satisfy canonical commutation relation

$$[a(l), a^*(k)] = \delta(k-l) \quad \text{for} \quad l, k \in \mathbb{R}^3 \tag{1.31}$$

The creation operator $a^*(k)$ adds a boson with momentum k, and the annihilation operator $a(k)$ removes a boson with momentum k. The operators $a(k)$ and $a^*(k)$ are actually *operator valued distributions*. When we smooth them out, we get a true operator:

$$a^*(f) = \int_{\mathbb{R}^3} f(k) a^*(k) d^3k$$

and

$$a(f) = \int_{\mathbb{R}^3} \bar{f}(k) a(k) d^3k,$$

where $f(k)$ is a wave function of a single boson.

Operator valued distribution means that the maps

$$f \mapsto \langle \psi_1, a(f)\psi_2 \rangle, \quad f \mapsto \langle \psi_1, a^*(f)\psi_2 \rangle$$

are distribution for all ψ_1, $\psi_2 \in \mathscr{H}_R$ in the common domain of all $a(f)$, $a^*(f)$.

The thermal equilibrium state is determined by the *two point function* (average)

$$\left\langle a^*(k)a(l) \right\rangle_\beta = \frac{\delta(k-l)}{e^{-\beta|k|} - 1} \tag{1.32}$$

(this is Planck's law of black-body radiation) and the property of *quasi-freeness*, which allows to express the averages of arbitrary products of creation and annihilation operators by just using the two-point function (1.32) (see [**32**]). The Hilbert space representation of the state $\langle \cdot \rangle_\beta$ is given by

$$\left\langle a^*(k)a(l) \right\rangle_\beta = \langle \Omega \otimes \Omega, a^*_\beta(k) a_\beta(l) \Omega \otimes \Omega \rangle, \tag{1.33}$$

where the inner product is that of $\mathscr{H}_R$, (1.26), and Ω is the vacuum vector. The positive temperature creation and annihilation operators are given by

$$\begin{aligned} a_\beta(k) &= \sqrt{1+\mu_\beta}\ \ a(k) \otimes \mathbb{I} + \sqrt{\mu_\beta}\ \ \mathbb{I} \otimes a^*(k), \\ a^*_\beta(k) &= \sqrt{1+\mu_\beta}\ \ a^*(k) \otimes \mathbb{I} + \sqrt{\mu_\beta}\ \ \mathbb{I} \otimes a(k), \end{aligned} \tag{1.34}$$

where μ_β is Planck's momentum density distribution for black-body radiation,

$$\mu_\beta(k) = \frac{1}{e^{\beta|k|} - 1}. \tag{1.35}$$

It is not hard to verify that, using (1.34) and (1.31), the right side of (1.33) equals the right side of (1.32).

In the scenario, the interaction operator between the system (spin chain) and a single reservoir (bose gas) is given by

$$\lambda \sigma^z \otimes \phi(g),$$

where $\lambda \in \mathbb{R}$ is a coupling constant, σ^z is the 2×2 Pauli spin matrix and $\phi(g)$ is the Bose field operator. This operator contains creation and annihilation operators, which physically describe processes of absorption and creation of reservoir quanta due to the interaction with the spin chain. The Bose field operator is smeared out with a coupling function or form factor $g(k) \in L^2(\mathbb{R}^3, d^3k)$, a wave function of a single boson. It contains an ultra-violet cut-off (cut-off for large $|k|$) and has the infra-red behaviour

$$0 < \lim_{|k| \to 0} \frac{|f(k)|}{|k|^p} = C < \infty. \tag{1.36}$$

In quantum-optical systems one has $p = 1/2$.

2. Model and Methodology

We consider an open quantum system consisting of a linear spin chain of three spins with nearest-neighbour Heisenberg-XX interactions, and two bosonic reservoirs connected with the linear spin chain. Figures 1.1 (left), 1.1 (middle) and 1.1 (right) represent the schematic diagrams of our model; the three spins are labeled by 1, 2 and 3, and two reservoirs are denoted as lower and upper reservoirs, respectively. The three spins are coupled to the lower and upper reservoirs. We first calculate the density matrix for the three spins, taking the trace over the two reservoirs. The diagonal elements of the density matrix represent the population of the states. Taking a further partial trace, we obtain the density matrix for spins 1 plus 2, for spins 1 plus 3, and for spins 1 and 2 alone.

2.1 Hamiltonian of the system

The total Hamiltonian of the system is given by

$$H = H_0 + H_1 \tag{2.1}$$

where

$$H_0 = -\hbar\omega \sum_{j=1}^{3} \sigma_j^z + \lambda_L \sum_{j=1}^{3} \sigma_j^z \otimes \varphi_L + \lambda_U \sum_{j=1}^{3} \sigma_j^z \otimes \varphi_U + H_L + H_U \tag{2.2}$$

and the interaction Hamiltonian [**33**]

$$H_1 = \frac{1}{2}\mu V, \qquad V = \sum_{i=1}^{2} (\sigma_i^x \sigma_{i+1}^x + \sigma_i^y \sigma_{i+1}^y). \tag{2.3}$$

Here, σ_i^α ($\alpha = x, y, z$) denotes the Pauli matrix σ^α acting only on the i-th spin. One can use the Heisenberg-XX interactions to transport quantum states, propagate and generate entanglement over the spin chain with minimal external control of the qubits [**5**, **33**, **34**]. The coefficient $\omega > 0$ is

the frequency of each spin; $\lambda_L \in \mathbb{R}$ and $\lambda_U \in \mathbb{R}$ are coupling constants; φ_L and φ_U are bosonic field operators for lower and upper reservoirs, respectively. The coefficient μ in equation (3) is the coupling constant between two consecutive spins. $H_{L/U}$ are the Hamiltonian of the lower and upper bosonic collective reservoirs, respectively, given by

$$H_{L/U} = \int_{\mathbb{R}^3} |k| a^*_{L/U}(k) a_{L/U}(k) d^3k, \tag{2.4}$$

and the bosonic field operators $\varphi_{L/U}$ are defined as

$$\varphi_{L/U} = \frac{1}{\sqrt{2}} \int_{\mathbb{R}^3} \{g_{L/U}(k) a^*_{L/U}(k) + g^*_{L/U}(k) a_{L/U}(k)\} d^3k \tag{2.5}$$

where $a_{L/R}(k)$ and $a^*_{L/R}(k)$ are annihilation and creation operators, respectively. Here $g_{L/U}$ is the form factor for lower (L) and upper (U) reservoir, respectively. For detailed description of the form factor one can see the section 1.7.

2.2 Density Matrix for three spins

Let $\rho(t)$ denote the density matrix of the entire system (three spins and two reservoirs) at time t. The reduced density matrix, $\rho^{123}(t)$ at time t, for the three spins alone, is

$$\rho^{123}(t) = Tr_R(\rho(t)). \tag{2.6}$$

Here Tr_R is the partial trace with respect to the reservoirs degrees of freedom, and the superscript 123 indicates the label of three spins in the linear spin chain. Using the time evolution operator we can rewrite the expression (2.6) as

$$\rho^{123}(t) = Tr_R(e^{-itH} \rho(0) e^{itH}). \tag{2.7}$$

For convenience, we have set $\hbar = 1$.

The initial state of the entire system $\rho(0)$ is assumed to be a product state of the form

$$\rho(0) = \rho^1(0) \otimes \rho^2(0) \otimes \rho^3(0) \otimes \rho^{R_L}(0) \otimes \rho^{R_U}(0) \tag{2.8}$$

where $\rho^{R_L}(0)$ and $\rho^{R_U}(0)$ are the initial states of the lower and upper reservoirs, respectively, and $\rho^i(0)$ ($i = 1,2,3$) is the initial state of the i-th spin, defined as

$$\rho^i(0) = \begin{pmatrix} p_i & v_i \\ v_i^* & 1-p_i \end{pmatrix} \tag{2.9}$$

with

$$0 \leq p_i \leq 1 \quad \text{and} \quad |v_i|^2 \leq p_i(1-p_i).$$

Theorem 2.2.1 — Commutator relation. The operators $H_\omega = \omega \sum_{i=1}^3 \sigma_i^z$ and $H_1 = J \sum_{j=1}^2 (\sigma_j^x \sigma_{j+1}^x + \sigma_j^y \sigma_{j+1}^y)$ satisfy $[H_1, H_\omega] = 0$.

Proof: Simplifying $[H_1, H_\omega]$, we obtain

$$\begin{aligned}
[H_1, H_\omega] &= [J\sum_{j=1}^{2}(\sigma_j^x\sigma_{j+1}^x + \sigma_j^y\sigma_{j+1}^y), \omega\sum_{i=1}^{3}\sigma_i^z] \\
&= J\omega\sum_{j=1}^{2}\sum_{i=1}^{3}[(\sigma_j^x\sigma_{j+1}^x + \sigma_j^y\sigma_{j+1}^y), \sigma_i^z] \\
&= J\omega\sum_{j=1}^{2}\sum_{i=1}^{3}\{[\sigma_j^x\sigma_{j+1}^x, \sigma_i^z] + [\sigma_j^y\sigma_{j+1}^y, \sigma_i^z]\} \\
&= J\omega\sum_{j=1}^{2}\sum_{i=1}^{3}\{\sigma_j^x[\sigma_{j+1}^x, \sigma_i^z] + [\sigma_j^x, \sigma_i^z]\sigma_{j+1}^x + \sigma_j^y[\sigma_{j+1}^y, \sigma_i^z] + [\sigma_j^y, \sigma_i^z]\sigma_{j+1}^y\} \quad (2.10)
\end{aligned}$$

We now use in (2.10) the commutator relation

$$[\sigma_k^x, \sigma_l^z] = -2i\sigma_k^y\delta_{kl}, \quad [\sigma_k^y, \sigma_l^z] = 2i\sigma_k^x\delta_{kl},$$

where δ_{kl} is the Kronecker symbol, to get

$$\begin{aligned}
[H_1, H_\omega] &= J\omega\sum_{j=1}^{2}\sum_{i=1}^{3}\{\sigma_j^x(-2i)\sigma_i^y\delta_{ij+1} + (-2i)\sigma_i^y\delta_{ij}\sigma_{j+1}^x + \sigma_j^y(2i)\sigma_i^x\delta_{ij+1} + (2i)\sigma_i^x\delta_{ij}\sigma_{j+1}^y\} \\
&= J\omega\sum_{j=1}^{2}\{\sigma_j^x(-2i)\sigma_{j+1}^y + (-2i)\sigma_j^y\sigma_{j+1}^x + \sigma_j^y(2i)\sigma_{j+1}^x + (2i)\sigma_j^x\sigma_{j+1}^y\}\} \\
&= \mathbf{0}. \quad (2.11)
\end{aligned}$$

This concludes the proof. ■

It follows from Theorem 2.2.1 and (2.2) that $[H_1, H_0] = \mathbf{0}$ so the equation (2.7) can be written as

$$\rho^{123}(t) = U(t)\Omega(t)U^*(t), \quad (2.12)$$

where $U(t) = e^{-itH_1}$ and

$$\Omega(t) = \mathrm{Tr}_R(e^{-itH_0}\rho(0)e^{itH_0}). \quad (2.13)$$

The evolution generated by the interaction Hamiltonian H_1 can be expressed as

$$U(t) = \exp[-i\frac{t\mu}{2}(\sigma_1^x\sigma_2^x + \sigma_1^y\sigma_2^y + \sigma_2^x\sigma_3^x + \sigma_2^y\sigma_3^y)]. \quad (2.14)$$

The following result will enable us to simplify $U(t)$.

Theorem 2.2.2 — Identity. The operators $\sigma_1^x\sigma_2^x + \sigma_2^y\sigma_3^y$ and $\sigma_1^y\sigma_2^y + \sigma_2^x\sigma_3^x$ commute, *i.e.*,

$$\left[\sigma_1^x\sigma_2^x + \sigma_2^y\sigma_3^y, \sigma_1^y\sigma_2^y + \sigma_2^x\sigma_3^x\right] = 0.$$

Proof: Simplifying $[\sigma_1^x\sigma_2^x + \sigma_2^y\sigma_3^y, \sigma_1^y\sigma_2^y + \sigma_2^x\sigma_3^x]$, we obtain

$$\begin{aligned}
&\left[\sigma_1^x\sigma_2^x + \sigma_2^y\sigma_3^y\ ,\ \sigma_1^y\sigma_2^y + \sigma_2^x\sigma_3^x\right] \\
&= [\sigma_1^x\sigma_2^x, (\sigma_1^y\sigma_2^y + \sigma_2^x\sigma_3^x)] + [\sigma_2^y\sigma_3^y, (\sigma_1^y\sigma_2^y + \sigma_2^x\sigma_3^x)] \\
&= [\sigma_1^x\sigma_2^x, \sigma_1^y\sigma_2^y] + [\sigma_1^x\sigma_2^x, \sigma_2^x\sigma_3^x] + [\sigma_2^y\sigma_3^y, \sigma_1^y\sigma_2^y] + [\sigma_2^y\sigma_3^y, \sigma_2^x\sigma_3^x] \quad (2.15)
\end{aligned}$$

The second and third commutator on the right hand side vanish, so

$$\begin{aligned}&\left[\sigma_1^x\sigma_2^x+\sigma_2^y\sigma_3^y\ ,\ \sigma_1^y\sigma_2^y+\sigma_2^x\sigma_3^x\right]\\ &= [\sigma_1^x\sigma_2^x,\sigma_1^y\sigma_2^y]+[\sigma_2^y\sigma_3^y,\sigma_2^x\sigma_3^x]\\ &= \sigma_1^x\sigma_1^y[\sigma_2^x,\sigma_2^y]+[\sigma_1^x,\sigma_1^y]\sigma_2^y\sigma_2^x+\sigma_2^y\sigma_2^x[\sigma_3^y,\sigma_3^x]+[\sigma_2^y,\sigma_2^x]\sigma_3^x\sigma_3^y.\end{aligned}$$

We use $[\sigma^x,\sigma^y]=2i\sigma^z$ and $\sigma^x\sigma^y=i\sigma^z$ to get

$$\begin{aligned}&\left[\sigma_1^x\sigma_2^x+\sigma_2^y\sigma_3^y\ ,\ \sigma_1^y\sigma_2^y+\sigma_2^x\sigma_3^x\right]\\ &= 2i\{\sigma_1^x\sigma_1^y\sigma_2^z+\sigma_1^z\sigma_2^y\sigma_2^x-\sigma_2^y\sigma_2^x\sigma_3^z-\sigma_2^z\sigma_3^x\sigma_3^y\}\\ &= 2i\{i\sigma_1^z\sigma_2^z-i\sigma_1^z\sigma_2^z+i\sigma_2^z\sigma_3^z-i\sigma_2^z\sigma_3^z\}\\ &= \mathbf{0}.\end{aligned}\tag{2.16}$$

This concludes the proof. ■

Using Theorem 2.2.2 we can rewrite (2.14) as [**35**]

$$U(t)=\exp[-\tfrac{1}{2}it\mu(\sigma_1^x\sigma_2^x+\sigma_2^y\sigma_3^y)]\times\exp[-\tfrac{1}{2}it\mu(\sigma_1^y\sigma_2^y+\sigma_2^x\sigma_3^x)].\tag{2.17}$$

The relations

$$\left(\tfrac{1}{\sqrt{2}}(\sigma_1^x\sigma_2^x+\sigma_2^y\sigma_3^y)\right)^2=I\ \text{ and }\ \left(\tfrac{1}{\sqrt{2}}(\sigma_1^y\sigma_2^y+\sigma_2^x\sigma_3^x)\right)^2=I,$$

where I is an identity operator, help us for further simplification, and the final form of the unitary operator is

$$\begin{aligned}U(t) &= [\cos(\alpha)I-\frac{i}{\sqrt{2}}\sin(\alpha)(\sigma_1^x\sigma_2^x+\sigma_2^y\sigma_3^y)]\times\\ &\quad [\cos(\alpha)I-\frac{i}{\sqrt{2}}\sin(\alpha)(\sigma_1^y\sigma_2^y+\sigma_2^x\sigma_3^x)],\end{aligned}\tag{2.18}$$

where

$$\alpha=\frac{t\mu}{\sqrt{2}}.$$

For the three spins, we consider the ordered basis

$$\left\{|000\rangle,|001\rangle,|010\rangle,|011\rangle,|100\rangle,|101\rangle,|110\rangle,|111\rangle\right\},\tag{2.19}$$

where $|0\rangle$ and $|1\rangle$ denote the spin down and up states (in the σ^z basis) respectively. The matrix form of the unitary operator $U(t)$ in the above ordered basis is given by

$$U(t)=\tag{2.20}$$

$$\begin{pmatrix}
1 & 0 & 0 & 0 & 0 & 0 & 0 & 0\\
0 & \cos^2\alpha & -\frac{i}{\sqrt{2}}\sin(2\alpha) & 0 & -\sin^2\alpha & 0 & 0 & 0\\
0 & -\frac{i}{\sqrt{2}}\sin(2\alpha) & \cos(2\alpha) & 0 & -\frac{i}{\sqrt{2}}\sin(2\alpha) & 0 & 0 & 0\\
0 & 0 & 0 & \cos^2\alpha & 0 & -\frac{i}{\sqrt{2}}\sin(2\alpha) & -\sin^2\alpha & 0\\
0 & -\sin^2\alpha & -\frac{i}{\sqrt{2}}\sin(2\alpha) & 0 & \cos^2\alpha & 0 & 0 & 0\\
0 & 0 & 0 & -\frac{i}{\sqrt{2}}\sin(2\alpha) & 0 & \cos(2\alpha) & -\frac{i}{\sqrt{2}}\sin(2\alpha) & 0\\
0 & 0 & 0 & -\sin^2\alpha & 0 & -\frac{i}{\sqrt{2}}\sin(2\alpha) & \cos^2\alpha & 0\\
0 & 0 & 0 & 0 & 0 & 0 & 0 & 1
\end{pmatrix}$$

Derivation of (2.20). The derivation of the explicit form (2.20) is straightforward. We illustrate it by showing how to get the first two rows. The matrix elements of $U(t)$, an 8×8 matrix, are defined by

$$[U(t)]_{mn} = \langle \alpha_1\alpha_2\alpha_3|U(t)|\beta_1\beta_2\beta_3\rangle, \quad m,n = 1,\ldots,8, \tag{2.21}$$

where

$$m = 1+2^2\alpha_1+2\alpha_2+\alpha_3 \ \text{ and } \ n = 1+2^2\beta_1+2\beta_2+\beta_3. \tag{2.22}$$

Here, α_i and β_i, for $i = 1,2,3$, are either 0 or 1.

$$\begin{aligned}
&\langle \alpha_1\alpha_2\alpha_3|U(t)|\beta_1\beta_2\beta_3\rangle \\
&= \langle \alpha_1\alpha_2\alpha_3|[\cos(\alpha)I - \frac{i}{\sqrt{2}}\sin(\alpha)(\sigma_1^x\sigma_2^x+\sigma_2^y\sigma_3^y)]\times \\
&\qquad [\cos(\alpha)I - \frac{i}{\sqrt{2}}\sin(\alpha)(\sigma_1^y\sigma_2^y+\sigma_2^x\sigma_3^x)]|\beta_1\beta_2\beta_3\rangle \\
&= \langle \alpha_1\alpha_2\alpha_3|[\cos(\alpha)I - \frac{i}{\sqrt{2}}\sin(\alpha)(\sigma_1^x\sigma_2^x+\sigma_2^y\sigma_3^y)]\times \\
&\qquad \{\cos(\alpha)|\beta_1\beta_2\beta_3\rangle - \frac{i}{\sqrt{2}}\sin(\alpha)(-(-1)^{\beta_1+\beta_2}|\bar\beta_1\bar\beta_2\beta_3\rangle + |\beta_1\bar\beta_2\bar\beta_3\rangle)\}
\end{aligned} \tag{2.23}$$

In equation (2.23), $|\bar\beta_i\rangle$ is the spin flip of the spin state $|\beta_i\rangle$, $|\bar 0\rangle = |1\rangle$ and $|\bar 1\rangle = |0\rangle$. After simplification we have

$$\begin{aligned}
&\langle \alpha_1\alpha_2\alpha_3|U(t)|\beta_1\beta_2\beta_3\rangle \\
&= \langle \alpha_1\alpha_2\alpha_3|[\{\cos^2(\alpha)+\frac{1}{2}(-1)^{\beta_1+\beta_2}\sin^2(\alpha)+\frac{1}{2}(-1)^{\bar\beta_2+\bar\beta_3}\sin^2(\alpha)\}|\beta_1\beta_2\beta_3\rangle \\
&\quad -\frac{i}{\sqrt{2}}\sin(\alpha)\cos(\alpha)(1-(-1)^{\beta_1+\beta_2})|\bar\beta_1\bar\beta_2\beta_3\rangle \\
&\quad -\frac{i}{\sqrt{2}}\sin(\alpha)\cos(\alpha)(1-(-1)^{\beta_2+\beta_3})|\beta_1\bar\beta_2\bar\beta_3\rangle \\
&\quad -\frac{1}{2}\sin^2(\alpha)(1-(-1)^{\bar\beta_2+\beta_3})|\bar\beta_1\beta_2\bar\beta_3\rangle].
\end{aligned} \tag{2.24}$$

The right hand side of the equation (2.24) is a combination of four different spin states; those are $|\beta_1\beta_2\beta_3\rangle$, $|\bar\beta_1\bar\beta_2\beta_3\rangle$, $|\beta_1\bar\beta_2\bar\beta_3\rangle$ and $|\bar\beta_1\beta_2\bar\beta_3\rangle$. Using the expression (2.24), we get

$$\begin{aligned}
&[U(t)]_{11} = 1, \ [U(t)]_{1n} = 0 \text{ for } n = 2,3,\ldots,8 \\
&[U(t)]_{22} = \cos^2(\alpha), \ [U(t)]_{23} = -\frac{i}{\sqrt{2}}\sin(2\alpha), \ [U(t)]_{25} = -\sin^2(\alpha) \text{ and} \\
&[U(t)]_{2n} = 0 \text{ for } n \neq 2,3,5.
\end{aligned} \tag{2.25}$$

This completes the derivation of how to get the first two rows of the matrix (2.20).

We see that $U(t) = I$ for $\alpha = n\pi$, $n = 0,1,\ldots$ Therefore, we get a collection of time-points

$$\tau_n = \frac{n\pi\sqrt{2}}{\mu}, \qquad n = 0,1,\ldots$$

at which the state of the system is the same as if it had evolved *without* spin-spin interaction (*i.e.*, for $H_1 = 0$).

To compute the density matrix $\rho^{123}(t)$, we have to evaluate the matrix elements of $\Omega(t)$, defined in equation (2.13), in the basis (2.19). $\Omega(t)$ is an 8×8 matrix with matrix elements defined by

$$[\Omega(t)]_{mn} = \langle \alpha_1\alpha_2\alpha_3|\mathrm{Tr}_R(e^{-itH_0}\rho(0)e^{itH_0})|\beta_1\beta_2\beta_3\rangle, \quad m,n=1,\dots,8, \tag{2.26}$$

where (according to the binary expansion)

$$m = 1+2^2\alpha_1+2\alpha_2+\alpha_3 \ \text{ and } \ n = 1+2^2\beta_1+2\beta_2+\beta_3. \tag{2.27}$$

Here, α_i and β_i, for $i=1,2,3$, are either 0 or 1.

To express the matrix elements in equation (2.27), we define the time-dependent decay rates

$$\Gamma_{L/U}(t) = \int_{\mathbb{R}^3} |g_{L/U}(k)|^2 \coth\Big(\frac{\beta_{L/U}|k|}{2}\Big)\frac{\sin^2(\frac{|k|t}{2})}{|k|^2}d^3k \tag{2.28}$$

and time-dependent phases

$$S_{L/U}(t) = \frac{1}{2}\int_{\mathbb{R}^3} |g_{L/U}(k)|^2 \frac{|k|t-\sin(|k|t)}{|k|^2}d^3k. \tag{2.29}$$

Theorem 2.2.3 — Matrix elements. For $m,n=1,\dots,8$ (with assocated α_j, β_j as per (2.27)), we have

$$\begin{aligned}
&[\Omega(t)]_{mn}\\
&= [\rho^1(0)\otimes\rho^2(0)\otimes\rho^3(0)]_{mn}\,\exp\Big[it\omega\sum_{j=1}^3\big((-1)^{\beta_j}-(-1)^{\alpha_j}\big)\Big]\\
&\quad\times\exp\Big[-\lambda_L^2\big(\sum_{j=1}^3(-1)^{\beta_j}-(-1)^{\alpha_j}\big)^2\Gamma_L(t)+i\lambda_L^2\big\{\big(\sum_{j=1}^3(-1)^{\alpha_j}\big)^2-\big(\sum_{j=1}^3(-1)^{\beta_j}\big)^2\big\}S_L(t)\Big]\\
&\quad\times\exp\Big[-\lambda_U^2\big(\sum_{j=1}^3(-1)^{\beta_j}-(-1)^{\alpha_j}\big)^2\Gamma_U(t)+i\lambda_U^2\big\{\big(\sum_{j=1}^3(-1)^{\alpha_j}\big)^2-\big(\sum_{j=1}^3(-1)^{\beta_j}\big)^2\big\}S_U(t)\Big].
\end{aligned} \tag{2.30}$$

Proof: Using the fact $\sigma^z|\beta\rangle = (-1)^{\beta+1}|\beta\rangle$, it follows from equations (2.26), (2.2) and (2.8)

$$\begin{aligned}
&[\Omega(t)]_{mn}\\
&= \exp\Big[it\omega\sum_{j=1}^3\big((-1)^{\beta_j}-(-1)^{\alpha_j}\big)\Big]\\
&\quad\times\mathrm{Tr}_L\Big\{\exp[-it\{\lambda_L\gamma_1\phi_L+H_L\}]\rho^{R_L}(0)\exp[it\{\lambda_L\gamma_2\phi_L+H_L\}]\Big\}\\
&\quad\times[\rho^1(0)\otimes\rho^2(0)\otimes\rho^3(0)]_{mn}\\
&\quad\times\mathrm{Tr}_U\Big\{\exp[-it\{\lambda_U\gamma_1\phi_U+H_U\}]\rho^{R_U}(0)\exp[it\{\lambda_U\gamma_2\phi_U+H_U\}]\Big\},
\end{aligned} \tag{2.31}$$

where

$$\gamma_1 = \sum_{j=1}^3(-1)^{\alpha_j+1} \qquad \text{and} \qquad \gamma_2 = \sum_{j=1}^3(-1)^{\beta_j+1}$$

and $\mathrm{Tr}_{L/U}$ are the traces with respect to the lower (L) and upper (U) reservoir degrees of freedom, respectively. It is well known that for $a,b\in\mathbb{R}$ (and $X=U,L$)

$$\begin{aligned}
&\mathrm{Tr}_X\Big\{\exp[-it\{a\phi_X+H_X\}]\rho^{R_X}(0)\exp[it\{b\phi_X+H_X\}]\Big\}\\
&\qquad = \exp\big[-i(a^2-b^2)S_X(t)-(a-b)^2\Gamma_X(t)\big],
\end{aligned} \tag{2.32}$$

where S and Γ are given in (2.28) and (2.29), see the proof of Proposition 7.7 in [**25**]. We combine (2.32) with (2.31) to obtain

$$\begin{aligned}
&[\Omega(t)]_{mn} \\
&= [\rho^1(0)\otimes\rho^2(0)\otimes\rho^3(0)]_{mn}\exp\Big[it\omega\sum_{j=1}^{3}\big((-1)^{\beta_j}-(-1)^{\alpha_j}\big)\Big] \\
&\quad\times\exp[i\lambda_L^2(\gamma_1^2-\gamma_2^2)S_L(t)-\lambda_L^2(\gamma_1-\gamma_2)^2\Gamma_L(t)] \\
&\quad\times\exp[i\lambda_U^2(\gamma_1^2-\gamma_2^2)S_U(t)-\lambda_U^2(\gamma_1-\gamma_2)^2\Gamma_U(t)].
\end{aligned} \tag{2.33}$$

This is the same as (2.30). ■

In (2.30), $[\rho^1(0)\otimes\rho^2(0)\otimes\rho^3(0)]_{mn}$ is the matrix element of the initial spin state (see (2.8)). The term $\exp[it\omega\sum_{j=1}^{3}((-1)^{\beta_j}-(-1)^{\alpha_j})]$ is generated by the dynamics in the absence of any interaction with the environments. The other two factors are decaying in time. Under suitable conditions on the infra-red ($k\approx 0$) behaviour of $g_{L/U}$ the 'time dependent decay rates' $\Gamma_U(t)$ and $\Gamma_L(t)$ become linear in t for large t [**25**]. The same holds for the phases $S_{L/U}(t)$.

2.3 Density Matrix for two spins

Let $\rho(t)$ denote the density matrix of the entire system (three spins and two reservoirs) at time t. The reduced density matrix, $\rho^{12}(t)$ and $\rho^{13}(t)$, of spins one and two and spins one and three, respectively, is

$$\rho^{12}(t)=\mathrm{Tr}_{3,R}(\rho(t))=\mathrm{Tr}_3(\rho^{123}(t)) \quad\text{and}\quad \rho^{13}(t)=\mathrm{Tr}_{2,R}(\rho(t))=\mathrm{Tr}_2(\rho^{123}(t)). \tag{2.34}$$

Here $\mathrm{Tr}_{3,R}$ is the partial trace over spin 3 and the reservoirs (and similarly for the other partial traces). The following matrices allow us to easily represent the reduced states $\rho^{12}(t)$ and $\rho^{13}(t)$,

$$A=\begin{pmatrix}1&0&0&0\\0&0&0&0\\0&1&0&0\\0&0&0&0\\0&0&1&0\\0&0&0&0\\0&0&0&1\\0&0&0&0\end{pmatrix}, \qquad A_{kl}=\delta_{k,2l-1} \tag{2.35}$$

$$B=\begin{pmatrix}0&0&0&0\\1&0&0&0\\0&0&0&0\\0&1&0&0\\0&0&0&0\\0&0&1&0\\0&0&0&0\\0&0&0&1\end{pmatrix}, \qquad B_{kl}=\delta_{k,2l} \tag{2.36}$$

$$G = \begin{pmatrix} 1 & 0 & 0 & 0 \\ 0 & 1 & 0 & 0 \\ 0 & 0 & 0 & 0 \\ 0 & 0 & 0 & 0 \\ 0 & 0 & 1 & 0 \\ 0 & 0 & 0 & 1 \\ 0 & 0 & 0 & 0 \\ 0 & 0 & 0 & 0 \end{pmatrix} \tag{2.37}$$

$$H = \begin{pmatrix} 0 & 0 & 0 & 0 \\ 0 & 0 & 0 & 0 \\ 1 & 0 & 0 & 0 \\ 0 & 1 & 0 & 0 \\ 0 & 0 & 0 & 0 \\ 0 & 0 & 0 & 0 \\ 0 & 0 & 1 & 0 \\ 0 & 0 & 0 & 1 \end{pmatrix} \tag{2.38}$$

One easily shows the following **properties of the matrices A, B, G and H**:

$$\begin{array}{ll} 1) & A^T A = B^T B = I_4, \\ 2) & AA^T + BB^T = I_8, \\ 3) & G^T G = H^T H = I_4, \\ 4) & GG^T + HH^T = I_8, \end{array}$$

where I_4 and I_8 are the identity matrices of order 4 and 8, respectively.

Theorem 2.3.1 — Structure of two spin density matrix. We have

$$\rho^{12}(t) = A^T \rho^{123}(t) A + B^T \rho^{123}(t) B, \tag{2.39}$$
$$\rho^{13}(t) = G^T \rho^{123}(t) G + H^T \rho^{123}(t) H, \tag{2.40}$$

where X^T is the transpose of a matrix X.

Proof: We derive (2.39). The relation (2.40) is obtained in a similar way. The elements of the matrix $\rho^{12}(t)$ can be written as

$$[\rho^{12}(t)]_{mn} = \langle \alpha_1 \alpha_2 | \rho^{12}(t) | \beta_1 \beta_2 \rangle, \tag{2.41}$$

where $m = 1 + 2\alpha_1 + \alpha_2$ and $n = 1 + 2\beta_1 + \beta_2$. We can rewrite (2.41) in terms of the three spin density matrix as (*c.f.* (2.34))

$$[\rho^{12}(t)]_{mn} = \sum_{\gamma=0,1} \langle \alpha_1 \alpha_2 \gamma | \rho^{123}(t) | \beta_1 \beta_2 \gamma \rangle. \tag{2.42}$$

Call the right hand side of (2.39) $S = A^T \rho^{123}(t) A + B^T \rho^{123}(t) B$. We calculate the matrix element

$$S_{mn} = \sum_{ij} \left\{ [A^T]_{mi} [\rho^{123}(t)]_{ij} [A]_{jn} + [B^T]_{mi} [\rho^{123}(t)]_{ij} [B]_{jn} \right\}. \tag{2.43}$$

Taking into account the definitions (2.35) and (2.36) yields

$$\begin{aligned} S_{mn} &= [\rho^{123}(t)]_{(2m-1)(2n-1)} + [\rho^{123}(t)]_{(2m)(2n)} \\ &= [\rho^{123}(t)]_{(1+4\alpha_1+2\alpha_2)(1+4\beta_1+2\beta_2)} + [\rho^{123}(t)]_{(1+4\alpha_1+2\alpha_2+1)(1+4\beta_1+2\beta_2+1)} \\ &= \langle \alpha_1\alpha_2 0|\rho^{123}(t)|\beta_1\beta_2 0\rangle + \langle \alpha_1\alpha_2 1|\rho^{123}(t)|\beta_1\beta_2 1\rangle \\ &= \sum_{\gamma=0,1} \langle \alpha_1\alpha_2\gamma|\rho^{123}(t)|\beta_1\beta_2\gamma\rangle. \end{aligned} \tag{2.44}$$

Combining (2.44) and (2.42) yields (2.39). ■

2.4 Density Matrix for single spin

Let $\rho(t)$ denote the density matrix of the entire system (three spins and two reservoirs) at time t. The reduced density matrix, $\rho^1(t)$ and $\rho^2(t)$, of spin one and two alone, respectively, is

$$\rho^1(t) = \mathrm{Tr}_{2,3,R}(\rho(t)) = \mathrm{Tr}_2(\rho^{12}(t)) \quad \text{and} \quad \rho^2(t) = \mathrm{Tr}_{1,3,R}(\rho(t)) = \mathrm{Tr}_1(\rho^{12}(t)). \tag{2.45}$$

The following matrices allow us to write $\rho^1(t)$ and $\rho^2(t)$ in a compact way,

$$\bar{A} = \begin{pmatrix} 1 & 0 \\ 0 & 0 \\ 0 & 1 \\ 0 & 0 \end{pmatrix}, \quad \bar{A}_{kl} = \delta_{k,2l-1} \tag{2.46}$$

$$\bar{B} = \begin{pmatrix} 0 & 0 \\ 1 & 0 \\ 0 & 0 \\ 0 & 1 \end{pmatrix}, \quad \bar{B}_{kl} = \delta_{k,2l} \tag{2.47}$$

$$\bar{G} = \begin{pmatrix} 1 & 0 \\ 0 & 1 \\ 0 & 0 \\ 0 & 0 \end{pmatrix}, \tag{2.48}$$

$$\bar{H} = \begin{pmatrix} 0 & 0 \\ 0 & 0 \\ 1 & 0 \\ 0 & 1 \end{pmatrix}. \tag{2.49}$$

One easily verifies the following **properties of the matrices $\bar{A}$, $\bar{B}$, $\bar{G}$ and $\bar{H}$**:

$$\begin{aligned} &1)\quad \bar{A}^T\bar{A} = \bar{B}^T\bar{B} = I_2, \\ &2)\quad \bar{A}\bar{A}^T + \bar{B}\bar{B}^T = I_4, \\ &3)\quad \bar{G}^T\bar{G} = \bar{H}^T\bar{H} = I_2, \\ &4)\quad \bar{G}\bar{G}^T + \bar{H}\bar{H}^T = I_4, \end{aligned}$$

where I_2 and I_4 are the identity matrices of order 2 and 4, respectively.

Theorem 2.4.1 — Structure of single spin density matrices. We have

$$\rho^1(t) = \bar{A}^T \rho^{12}(t)\bar{A} + \bar{B}^T \rho^{12}(t)\bar{B}, \tag{2.50}$$
$$\rho^2(t) = \bar{G}^T \rho^{12}(t)\bar{G} + \bar{H}^T \rho^{12}(t)\bar{H}. \tag{2.51}$$

Proof: We show how to get (2.50). Then (2.51) is derived in the same way. The elements of the matrix $\rho^{12}(t)$ can be written as

$$[\rho^1(t)]_{mn} = \langle \alpha_1 | \rho^1(t) | \beta_1 \rangle, \tag{2.52}$$

where $m = 1 + \alpha_1$ and $n = 1 + \beta_1$. We can rewrite (2.52) in terms of the two-spin density matrix as (*c.f.* (2.45))

$$[\rho^1(t)]_{mn} = \sum_{\gamma=0,1} \langle \alpha_1 \gamma | \rho^{12}(t) | \beta_1 \gamma \rangle. \tag{2.53}$$

Call the right hand side of (2.50) $S = \bar{A}^T \rho^{12}(t)\bar{A} + \bar{B}^T \rho^{12}(t)\bar{B}$. We calculate the matrix element

$$S_{mn} = \sum_{ij} \left\{ [\bar{A}^T]_{mi} [\rho^{12}(t)]_{ij} [\bar{A}]_{jn} + [\bar{B}^T]_{mi} [\rho^{12}(t)]_{ij} [\bar{B}]_{jn} \right\}. \tag{2.54}$$

Taking into account the definitions (2.46) and (2.47) yields

$$\begin{aligned} S_{mn} &= [\rho^{12}(t)]_{(2m-1)(2n-1)} + [\rho^{12}(t)]_{(2m)(2n)} \\ &= [\rho^{12}(t)]_{(1+2\alpha_1)(1+2\beta_1)} + [\rho^{12}(t)]_{(1+2\alpha_1+1)(1+2\beta_1+1)} \\ &= \langle \alpha_1 0 | \rho^{12}(t) | \beta_1 0 \rangle + \langle \alpha_1 1 | \rho^{12}(t) | \beta_1 1 \rangle \\ &= \sum_{\gamma=0,1} \langle \alpha_1 \gamma | \rho^{12}(t) | \beta_1 \gamma \rangle. \end{aligned} \tag{2.55}$$

Combining (2.55) and (2.53) yields (2.50). ■

In the following result, we verify explicitly that the reduced density matrices are normalized correctly.

Theorem 2.4.2 We have, for all t,

$$\mathrm{Tr}(\rho^{123}(t)) = \mathrm{Tr}(\rho^{12}(t)) = \mathrm{Tr}(\rho^1(t)) = 1. \tag{2.56}$$

Proof: We will not write the time dependence explicitly. It follows from equation (2.12) that

$$[\rho^{123}]_{ii} = \sum_{mn} U_{im} \Omega_{mn} [U^*]_{ni}. \tag{2.57}$$

Therefore,

$$\begin{aligned} \mathrm{Tr}(\rho^{123}) &= \sum_{i=1}^{8} \sum_{mn} U_{im} \Omega_{mn} [U^*]_{ni} \\ &= \sum_{mn} \Big(\sum_{i=1}^{8} U_{im} [U^*]_{ni} \Big) \Omega_{mn}. \end{aligned} \tag{2.58}$$

Since U is unitary, we have $[U^*U]_{nm} = \delta_{n,m}$, so

$$\mathrm{Tr}(\rho^{123}) = \sum_{m} \Omega_{mm} = \mathrm{Tr}_{1,2,3}\,\Omega = \mathrm{Tr}_{1,2,3,R}(e^{-itH_0} \rho(0) e^{itH_0}) = \mathrm{Tr}_{1,2,3,R}(\rho(0)) = 1. \tag{2.59}$$

In the third equality, we used the definition of Ω, (2.13).

Now we verify that $\mathrm{Tr}(\rho^{12}) = 1$. We have

$$\mathrm{Tr}(\rho^{12}) = \langle 00|\rho^{12}|00\rangle + \langle 01|\rho^{12}|01\rangle + \langle 10|\rho^{12}|10\rangle + \langle 11|\rho^{12}|11\rangle. \tag{2.60}$$

We can rewrite (2.60) in terms of ρ^{123} and simplify,

$$\begin{aligned}\mathrm{Tr}(\rho^{12}) &= \sum_{i=0,1}\Big[\langle 00i|\rho^{123}|00i\rangle + \langle 01i|\rho^{123}|01i\rangle + \langle 10i|\rho^{123}|10i\rangle + \langle 11i|\rho^{123}|11i\rangle\Big] \\ &= \sum_{i=1}^{8}[\rho^{123}]_{ii} \\ &= \mathrm{Tr}(\rho^{123}) \\ &= 1. \end{aligned} \tag{2.61}$$

Similarly,

$$\mathrm{Tr}(\rho^{1}) = \langle 0|\rho^{1}|0\rangle + \langle 1|\rho^{1}|1\rangle = \sum_{i=0,1}\big[\langle 0i|\rho^{12}|0i\rangle + \langle 1i|\rho^{12}|1i\rangle\big] = \sum_{i=1}^{4}[\rho^{12}]_{ii} = \mathrm{Tr}(\rho^{12}) = 1.$$

This finishes the proof. ■

2.5 Entanglement

Entanglement is a notion of quantum correlation between two (several) components of a composite system. Consider a composite system of two subsystems A and B, each associated with a Hilbert space $\mathscr{H}_A$ and $\mathscr{H}_B$, respectively. Let $|\psi_{AB}\rangle \in \mathscr{H}_{AB} := \mathscr{H}_A \otimes \mathscr{H}_B$ be a state of the composite system.

We say that $|\psi_{AB}\rangle$ is *disentangled* (not entangled, a product state) if $|\psi_{AB}\rangle$ can be expressed as a product of two states $|\psi_A\rangle \in \mathscr{H}_A$ and $|\psi_B\rangle \in \mathscr{H}_B$, *i.e.*, $|\psi_{AB}\rangle = |\psi_A\rangle \otimes |\psi_B\rangle$. The state of the composite system $|\psi_{AB}\rangle$ is called *entangled* when it is not possible to express $|\psi_{AB}\rangle$ as such a product.

■ **Example 2.1** The Bell states are examples of entangled two-qubit states. Consider the Bell state

$$|\psi_{12}\rangle = \frac{1}{\sqrt{2}}\big(|00\rangle + |11\rangle\big) \tag{2.62}$$

In trying to write $|\psi_{12}\rangle$ as a product state, make the Ansatz

$$|\psi_1\rangle = a_1|0\rangle + b_1|1\rangle$$

and

$$|\psi_2\rangle = a_2|0\rangle + b_2|1\rangle.$$

Therefore,

$$|\psi_1\rangle \otimes |\psi_2\rangle = a_1a_2|00\rangle + a_1b_2|01\rangle + a_2b_1|10\rangle + b_1b_2|11\rangle$$

Now

$$|\psi_{12}\rangle = |\psi_1\rangle \otimes |\psi_2\rangle \Rightarrow a_1a_2 = 1/\sqrt{2},\ \ a_1b_2 = 0,\ \ a_2b_1 = 0 \ \text{ and } \ b_1b_2 = 1/\sqrt{2}.$$

It is not possible to find numbers satisfying this, so we can not express $|\psi_{12}\rangle$ as a product state. Thus it is entangled. ■

■ **Example 2.2** The pure state $|01\rangle$ is a non-entangled state since we can express the state in product form

$$|01\rangle = |0\rangle \otimes |1\rangle. \tag{2.63}$$

■

If a bipartite, composite system $A+B$ is in a disentangled state $|\psi\rangle$, then the two subsystems are not correlated (independent), in the following sense. Upon measuring any two quantities, one on system A and one on system B, according to the fundamental postulates of quantum theory, the outcome results are two random variables. If the state is not entangled, then those random variables are *independent* (in the usual sense of probability theory).

■ **Example 2.3 entanglement and correlation.** Consider the pure state

$$|\psi\rangle = \frac{\sqrt{3}}{2}|00\rangle + \frac{1}{2}|11\rangle \tag{2.64}$$

One can check that this state is entangled, just as we did above for the Bell state (2.62). Upon measuring the spin 1, the possible outcome is 0 or 1 (same for spin 2). The probability of getting the outcome 0 when making a measurement on the first spin in the composite state (2.64) equals $3/4$. If the measurement out come is 0 for this measurement, then, by the principles of quantum theory (collapse of the wave function), the wave function (2.64) immediately after the measurement is $|\psi'\rangle = |00\rangle$. (If the value 1 was the outcome – which happens with probability $1/4$, then the post measurement state would be $|11\rangle$). After the first measurement, the state is thus $|00\rangle$ or $|11\rangle$, *depending* on the outcome of the first measurement. Now we perform a second measurement, on spin 2. If 0 was measured previously on spin 1, then with probability equal to 1, the outcome on the spin 2 measurement will be the value 0. Conversely, if the value 1 was measured for spin 1, then with certainty, the second measurement for spin 2 will yield the result 1. *Therefore, the measurement outcome on spin 2 is correlated (to '100%') with that of spin 1.*

On the other hand, consider the disentangled state

$$|\psi\rangle = \Big(\frac{1}{4}|0\rangle + \frac{\sqrt{15}}{4}|1\rangle\Big) \otimes \Big(\frac{1}{3}|0\rangle + \frac{\sqrt{8}}{3}|1\rangle\Big). \tag{2.65}$$

If the value 0 or 1 is measured on spin 1 (which happens with probability $1/16$ and $15/16$, respectively), then the post measurement state is

$$|0\rangle \otimes \Big(\frac{1}{3}|0\rangle + \frac{\sqrt{8}}{3}|1\rangle\Big) \quad \text{or} \quad |1\rangle \otimes \Big(\frac{1}{3}|0\rangle + \frac{\sqrt{8}}{3}|1\rangle\Big), \tag{2.66}$$

respectively. Any measurement on spin 2 is now *independent* of which of the two states (2.66) we are dealing with (as the second factor is the same). So the measurement outcome on spin 2 is *independent* of the spin 1 measurement outcome in the *disentangled* state (2.65). ■

The notion of entanglement is generalized to mixed states as follows. Suppose A and B are globally prepared in a mixed state, described by a density matrix $\rho_{AB} \in \mathscr{D}_{AB}$ where $\mathscr{D}_{AB}$ is the convex set of all density operators acting on the Hilbert space $\mathscr{H}_{AB}$. The state ρ_{AB} is called *separable* [**36**] if we can express ρ_{AB} as

$$\rho_{AB} = \sum_i p_i \rho_A^{(i)} \otimes \rho_B^{(i)}, \tag{2.67}$$

where p_i is a probability distribution, and $\{\rho_A^{(i)}\}$ and $\{\rho_B^{(i)}\}$ are states of the subsystems A and B, respectively. A mixed state which is not separable is called *entangled*.

The *von Neumann entropy* of a state ρ is defined by

$$S(\rho) = -\mathrm{Tr}(\rho \log_2 \rho) \geq 0 \tag{2.68}$$

where Tr denotes the trace.

Theorem 2.5.1 The von Neumann entropy is a good measure of purity, since

$$\rho \text{ is pure} \iff S(\rho) = 0$$

Proof: We can rewrite the expression (2.68) as

$$S(\rho) = -\sum_j \lambda_j \log_2 \lambda_j, \tag{2.69}$$

where λ_j are the eigenvalues of the density matrix ρ. Note that since $\lambda \in [0,1]$, we have $-\lambda \log_2 \lambda \geq 0$ with equality if and only if $\lambda \in \{0,1\}$. Assume that ρ is pure. This means ρ is a projection, so its eigenvalues are only 0 or 1. So $S(\rho) = 0$. Conversely, suppose $S(\rho) = 0$. Since $S(\rho)$ is a sum of non-negative terms, this implies that each term in the sum must vanish. Therefore, all eigenvalues λ of ρ are either 0 or 1. However, since $\mathrm{Tr}(\rho) = 1$, there is exactly *one* eigenvalue 1 and all others must be zero. Consequently, ρ is a rank-one projection, so, a pure state. ■

■ **Example 2.4** Consider the pure state

$$|\psi_1\rangle = \frac{1}{\sqrt{2}}(|0\rangle + |1\rangle) \tag{2.70}$$

where $|0\rangle$ and $|1\rangle$ represent spin down and spin up states, respectively. The density matrix corresponding the pure state $|\psi_1\rangle$ is given by

$$\rho_1 = \frac{1}{2}\begin{pmatrix} 1 & 1 \\ 1 & 1 \end{pmatrix}. \tag{2.71}$$

The eigenvalues of the density matrix ρ_1 are 0 and 1 so

$$S(\rho_1) = 0$$

■

■ **Example 2.5** Consider the mixed state represented by the density matrix ρ_m where

$$\rho_m = \begin{pmatrix} 0.66 & 0.28 \\ 0.28 & 0.34 \end{pmatrix}. \tag{2.72}$$

The eigenvalues of the density matrix ρ_m are 0.1775 and 0.8225 so $S(\rho_m) = 0.6746$ bits. ■

Let $|\psi_{AB}\rangle$ be a pure state of the composite system $A+B$. Using partial trace, the reduced states of the subsystems A and B are defined by

$$\rho_A = \mathrm{Tr}_B |\psi_{AB}\rangle\langle\psi_{AB}|$$

and

$$\rho_B = \mathrm{Tr}_A |\psi_{AB}\rangle\langle\psi_{AB}|$$

The relation between entanglement and purity is given below:

Theorem 2.5.2 For a pure state $|\psi_{AB}\rangle$ of the composite system A+B,

$$\rho_A \quad \text{is pure} \iff |\psi_{AB}\rangle \quad \text{is not entangled.}$$

Proof: The density matrix of the composite system can be written as

$$\rho_{AB} = |\psi_{AB}\rangle\langle\psi_{AB}| \tag{2.73}$$

Expand $|\psi_{AB}\rangle$ to the spectral basis of ρ_A, $\{u_i\}$, and ρ_B, $\{v_j\}$, we have

$$|\psi_{AB}\rangle = \sum_{ij} C_{ij}|u_i v_j\rangle \tag{2.74}$$

Using the expantion (2.74), we can rewrite the (2.73) as

$$\begin{aligned}\rho_{AB} &= \sum_{ij}\sum_{kl} C_{ij}\overline{C_{kl}}|u_i v_j\rangle\langle u_k v_l| \\ &= \sum_{ij}\sum_{kl} C_{ij}\overline{C_{kl}}|u_i\rangle\langle u_k| \otimes |v_j\rangle\langle v_l|\end{aligned} \tag{2.75}$$

Using the partial trace, we can obtain the reduced density matrix ρ_A as

$$\begin{aligned}\rho_A &= \mathrm{Tr}_B(\rho_{AB}) \\ &= \sum_{ij}\sum_{kl} C_{ij}\overline{C_{kl}}|u_i\rangle\langle u_k|\langle v_j|v_l\rangle \\ &= \sum_{ijk} C_{ij}\overline{C_{kj}}|u_i\rangle\langle u_k|\end{aligned} \tag{2.76}$$

Assume that ρ_A is a pure state. Since $\{u_i\}$ is the eigenbasis of ρ_A, we can assume without loss of generality that

$$\rho_A = |u_1\rangle\langle u_1| \tag{2.77}$$

It follows from equations (2.76)

$$|u_1\rangle\langle u_1| = \sum_{ijk} C_{ij}\overline{C_{kj}}|u_i\rangle\langle u_k| \tag{2.78}$$

The coefficient of $|u_\ell\rangle\langle u_\ell|$ on the right side is $\sum_j |C_{\ell j}|^2$ and so we have from (2.78) that

$$\sum_j |C_{1j}|^2 = 1 \qquad \text{and} \qquad \sum_j |C_{\ell j}|^2 = 0 \quad \forall \ell > 1 \tag{2.79}$$

(2.79) gives $C_{\ell j} = 0$ if $\ell > 1$, for all j. Using this in (2.75) we obtain

$$\begin{aligned}\rho_{AB} &= \sum_{j,l} C_{1j}\overline{C_{1l}}|u_1\rangle\langle u_1| \otimes |v_j\rangle\langle v_l| \\ &= |u_1\rangle\langle u_1| \otimes \sum_{j,l} C_{1j}\overline{C_{1l}}|v_j\rangle\langle v_l| \qquad (2.80) \\ &= |u_1\rangle\langle u_1| \otimes \Big|\sum_j C_{1j}v_j\Big\rangle\Big\langle\sum_j C_{1j}v_j\Big| \qquad (2.81)\end{aligned}$$

which is a pure product state of the form $|\psi_{AB}\rangle = |u_1 \otimes (\sum_j C_{1j}v_j)\rangle$.

Conversely, suppose that $|\psi_{AB}\rangle$ is not entangled. So by definition $|\psi_{AB}\rangle = |u\rangle \otimes |v\rangle$ for some vectors u, v. Then of course,

$$\rho_A = \mathrm{Tr}_B(|u\rangle \otimes |v\rangle)(\langle u| \otimes \langle v|) = \mathrm{Tr}_B(|u\rangle\langle u| \otimes |v\rangle\langle v|) = |u\rangle\langle u|,$$

which is a pure state. ■

To investigate the entanglement of the present system, we consider the following measures: the *concurrence* between two qubits and the concurrence between a single qubit and two other ones, and the *intrinsic three particle entanglement*.

2.5.1 Concurrence between two qubits

Let ρ be a density matrix of 2 qubits, and the corresponding 'spin-flipped' density matrix $\widetilde{\rho}$ is defined as

$$\widetilde{\rho} = (\sigma^y \otimes \sigma^y)\rho^*(\sigma^y \otimes \sigma^y), \tag{2.82}$$

where ρ^* is complex conjugate of ρ and σ^y is a Pauli spin matrix.

The concurrence of those 2 qubits can be defined as

$$C(\rho) = \max\{\lambda_1 - \lambda_2 - \lambda_3 - \lambda_4, 0\}, \tag{2.83}$$

where λ_1, λ_2, λ_3 and λ_4 are the square root of the eigenvalues, in decreasing order, of the Hermitian matrix $\sqrt{\rho}\widetilde{\rho}\sqrt{\rho}$.

The concurrence C_{ij}, the measure of bipartite entanglement between i-th and j-th qubits, can be defined as [**37**]

$$C_{ij}(t) = \max\{\lambda_1 - \lambda_2 - \lambda_3 - \lambda_4, 0\}, \tag{2.84}$$

where λ_1, λ_2, λ_3 and λ_4 are the square root of the eigenvalues, in decreasing order, of $\rho^{ij}(t)\widetilde{\rho^{ij}(t)}$, the product of density matrix and 'spin-flipped' density matrix. Here, $\rho^{ij}(t)$ is the density matrix of the pair of qubits, i-th and j-th, and the 'spin-flipped' density matrix $\widetilde{\rho^{ij}(t)}$ is defined as

$$\widetilde{\rho^{ij}(t)} = (\sigma^y \otimes \sigma^y)[\rho^{ij}(t)]^*(\sigma^y \otimes \sigma^y), \tag{2.85}$$

where the asterisk denotes complex conjugate, and σ^y is the Pauli matrix. It should noticed that both the operators $\rho^{ij}(t)$ and $\widetilde{\rho^{ij}(t)}$ are positive so their product $\rho^{ij}(t)\widetilde{\rho^{ij}(t)}$, although non-Hermitian, has merely real and positive eigenvalues. The values of the concurrence $C_{ij}(t)$ lies between 0 and 1, and $C_{ij}(t) = 0$ indicates that the states of two qubits are separable while the states of two qubits are maximally entangle is represented by $C_{ij}(t) = 1$.

Theorem 2.5.3 Let ρ be a density matrix (of any finite dimensional quantum system) and let A be a hermitian, positive definite matrix. We have

$$(i) \quad \rho A \text{ and } \sqrt{\rho}A\sqrt{\rho} \text{ have the same eigenvalues.} \tag{2.86}$$

$$(ii) \quad \sqrt{\rho}A\sqrt{\rho} \text{ is Hermitian.} \tag{2.87}$$

$$(iii) \quad \sqrt{\rho}A\sqrt{\rho} \text{ is positive definite.} \tag{2.88}$$

Remark: $A = \widetilde{\rho}$, as defined in (2.82) is hermitian and positive definite.

Proof of Theorem 2.5.3. (i) We know that if M and N are square matrices of the same size then MN and NM have the same characteristic polynomial [**38**]. Suppose $M = \sqrt{\rho}A$ and $N = \sqrt{\rho}$ so $MN = \sqrt{\rho}A\sqrt{\rho}$ and $NM = \rho A$. Therefore, ρA and $\sqrt{\rho}A\sqrt{\rho}$ have the same characteristic polynomials which implies that ρA and $\sqrt{\rho}A\sqrt{\rho}$ have the same eigenvalues.

This proves (i).

To prove (ii) we notice that $(\sqrt{\rho}A\sqrt{\rho})^* = \sqrt{\rho}A^*\sqrt{\rho}$, so the hermiticity of this product follows directly from that of A.

To prove (iii) we notice that since $\sqrt{\rho}$ is a positive operator, positivity of A is equivalent to that of $\sqrt{\rho}A\sqrt{\rho}$. This concludes the proof of Theorem 2.5.3 ■

2.5.2 Concurrence in three qubits

For a tripartite system, the concurrence between a qubit i and rest of the system, qubits j and k, can be defined as [**39**]

$$C_{i(jk)}(t) = \sqrt{2\{1 - \mathrm{Tr}([\rho^i(t)]^2)\}}, \tag{2.89}$$

where $\mathrm{Tr}([\rho^i(t)]^2)$ is the trace of the square of the reduced density matrix $\rho^i(t)$.

2.5.3 Intrinsic three particle entanglement

The essential three-way entanglement of the tripartite system, qubits i, j and k can be written as [**40**]

$$C_{ijk} = C^2_{i(jk)} - C^2_{ij} - C^2_{ik}. \tag{2.90}$$

It follows from the above expression that the essential entanglement of i, j, k is a quadratic combination of the entanglement of i with jk, the entanglement of i with j and the entanglement of i with k.

3. Numerical Results

For computational purposes, we use dimensionless parameters and variables by introducing a characteristic frequency, ω_0, typically of the order of the spin transition frequency ω, see (2.2). The total Hamiltonian, energies of the spin states, and temperature are measured in $\hbar\omega_0$ unit. According to [**41**] we choose the form factors $g_{L/R}(k)$ (see (2.5)) as

$$|g_{L/U}(k)|^2 = |k|e^{-|k|/\varkappa_{L/U}}, \tag{3.1}$$

where $\varkappa_{L/U} > 0$ is a suitable ultraviolet cut-off. We consider the cut-off frequency equal to the thermal frequency of the reservoir given by

$$\varkappa_{L/U} = \frac{k_B T_{L/U}}{h}, \tag{3.2}$$

where k_B is the Boltzmann constant, and $T_{L/U}$ are the temperature of the lower and upper reservoirs, respectively. We introduce a scaling time $t_0 = \frac{1}{\mu} t\omega_0$ where $t\omega_0$ is the dimensionless time and μ is the spin-spin coupling constant.

In all numerical calculations performed in this thesis, we take $|v_j|$, the off-diagonal density matrix elements in the initial spin states, defined in expression (2.9), to be equal to 96% of p_i,

$$|v_j| = 0.96 p_j \tag{3.3}$$

As it turns out, and we have checked this numerically, the phase of the complex numbers v_j does not affect the various curves for the entanglement. Therefore, (3.3) suffices to determine the initial spin state for our purposes. We take $|v_j|$ close to p_j since this favours larger entanglement creation [**41**].[1]

We divide our calculated results into three parts: **no coupling to reservoirs, coupling to a single reservoir and to two reservoirs**. In the next three sections we describe the numerical results for the present system.

[1] Note: we always have the constraint $|v|^2 \leq p(1-p)$ as v and p must define a density matrix. Then $|v|^2 = (0.96)^2 p^2$ gives the condition $p \leq \frac{1}{1+(0.96)^2} \approx 0.52$.

3.1 Dynamics of the chain without coupling to reservoirs

In this section, we consider the 3-spin density matrix, written in the energy basis (the basis diagonalizing the σ_z, i.e., $|0\rangle$, $|1\rangle$) and we analyze the dynamics of the populations, i.e., the diagonal density matrix elements.

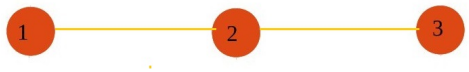

Figure 3.1: A schematic representation of the present system. The spin chain of three spins, labelled 1, 2 and 3, respectively.

Recall that the initial population of spin j in level $|0\rangle$ is p_j. We consider four sets of values,

$$(p_1,p_2,p_3) = (0.2,0.2,0.2),\ (0.2,0.2,0.4),\ (0.2,0.3,0.4),\ (0.3,0.5,0.5) \equiv S1,S2,S3,S4. \quad (3.4)$$

We also study numerically the concurrences.

3.1.1 Population Analysis: Figures 3.2 – 3.5

The diagonal elements of three-spin density matrix $[\rho^{123}(t)]_{11}$ and $[\rho^{123}(t)]_{88}$ represent the population of the two ferromagnetic states $|000\rangle$ and $|111\rangle$, respectively, which are constant,

$$[\rho^{123}(t)]_{11} = p_1p_2p_3, \quad [\rho^{123}(t)]_{88} = (1-p_1)(1-p_2)(1-p_3).$$

To see that these populations are indeed constant in time, we recall from expression (2.12) that

$$[\rho^{123}(t)]_{\ell\ell} = \sum_{mn}[U(t)]_{\ell m}[\Omega(t)]_{mn}[U^*(t)]_{n\ell}, \qquad \ell = 1,8 \quad (3.5)$$

The explicit form of the matrix (2.20), shows that $[U(t)]_{1m} \neq 0$ for $m = 1$ only, and $[U(t)]_{11} = 1$, and that $[U^*(t)]_{n1} \neq 0$ for $n = 1$ only and $[U^*(t)]_{11} = 1$. Therefore (3.5) for $\ell = 1$ reduces to

$$[\rho^{123}(t)]_{11} = [U(t)]_{11}[\Omega(t)]_{11}[U^*(t)]_{11} = [\Omega(t)]_{11} \quad (3.6)$$

According to (2.30), we have (see also (2.9))

$$[\Omega(t)]_{11} = [\rho^1(0)\otimes\rho^2(0)\otimes\rho^3(0)]_{11} = p_1p_2p_3$$

The argument for $\ell = 8$ is the same.

The antiferromagnetic states $|001\rangle$ and $|100\rangle$ have the same populations. The states $|011\rangle$ and $|110\rangle$ do as well. In Figures 3.2 – 3.5, we show the populations of the states $|001\rangle$, $|010\rangle$, $|011\rangle$ and $|101\rangle$. They are given by the diagonal elements $[\rho^{123}(t)]_{22}$, $[\rho^{123}(t)]_{33}$, $[\rho^{123}(t)]_{44}$ and $[\rho^{123}(t)]_{66}$, respectively.

The figures reveal the following facts.

- Figure 3.1 shows that for most times, the population is lowest for S1, increases for S2 and S3, and finally is highest for S4. The maximum value of $[\rho^{123}(t)]_{22}$ for S4 is significantly higher than that of for the other sets.
- The graphs in Figure 3.2. show a similar behaviour, for the state $|010\rangle$.
- It follows from figure 3.3 that the population of the spin state $|011\rangle$ is minimum for S2 and maximum for S2 as well. The other three sets produce intermediate populations. The difference between two consecutive maximum values of $[\rho^{123}(t)]_{44}$ for S2, S3, S4 and S1 are almost the same.

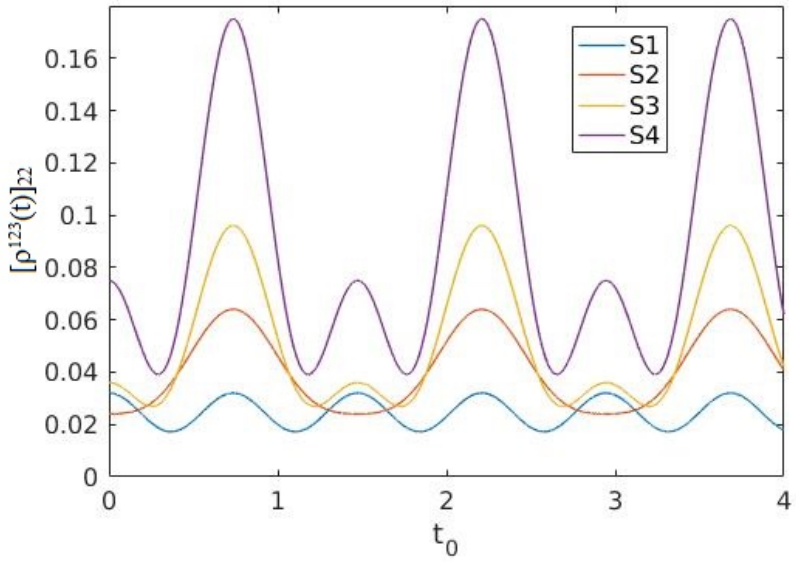

Figure 3.2: The diagonal element $[\rho^{123}(t)]_{22}$ as a function of the scaling time t_0 for the four different sets of p_j, (3.4).

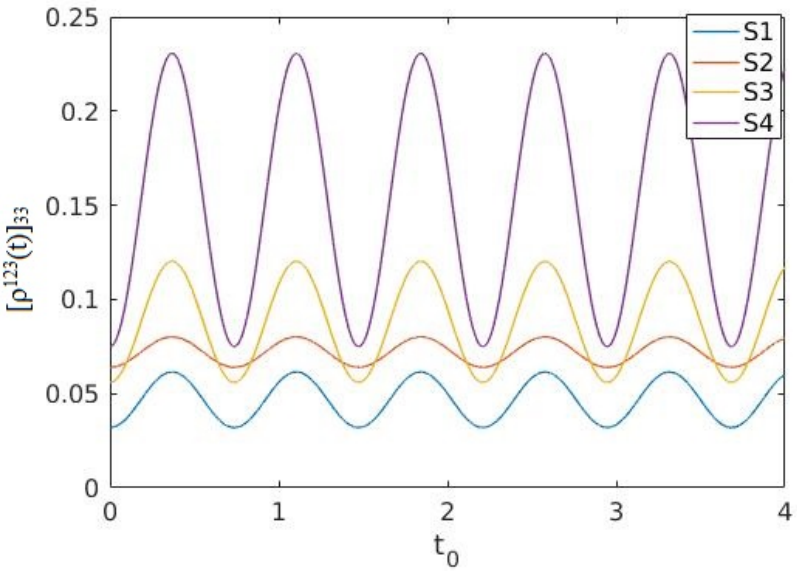

Figure 3.3: The diagonal element $[\rho^{123}(t)]_{33}$ as a function of the scaling time t_0 for the S_j in (3.4)

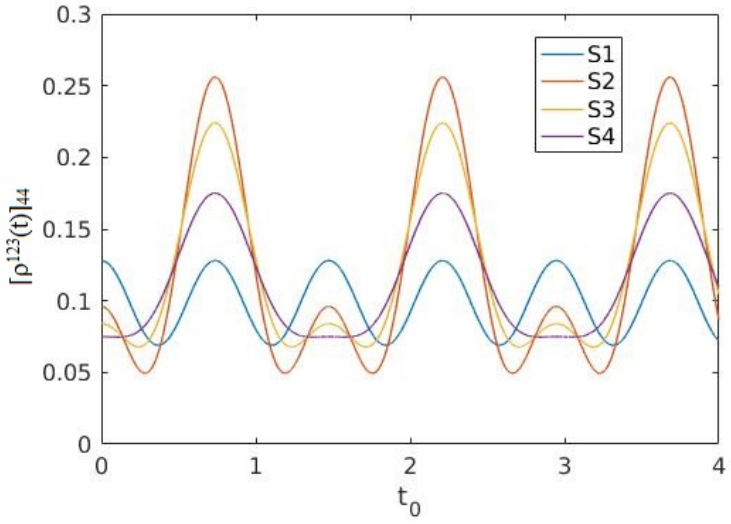

Figure 3.4: The diagonal element $[\rho^{123}(t)]_{44}$ as a function of the scaling time t_0 for the S_j in (3.4)

- In Figure 3.4, we observe a similar phenomenon as Figure 3.3, although there is some difference. Namely, the population curves for S2 and S4 are symmetrical with respect to the horizontal line $[\rho^{123}(t)]_{66} = 0.22$.

The analytical description of the quantities graphed in this section is as we now describe for $[\rho^{123}(t)]_{22}$ (corresponding to Fig. 3.1). We obtain from the matrix (2.20) the relations

$$\text{For} \quad i = 2,3,5 \quad [U(t)]_{im} \neq 0 \quad \text{and} \quad [U^*(t)]_{mi} \neq 0 \quad \text{when} \quad m = 2,3,5$$

and

$$\text{For} \quad i = 4,6,7 \quad [U(t)]_{im} \neq 0 \quad \text{and} \quad [U^*(t)]_{mi} \neq 0 \quad \text{when} \quad m = 4,6,7.$$

Then (2.12) simplifies to

$$\begin{aligned}
[\rho^{123}(t)]_{22} &= \sum_{mn} [U(t)]_{2m}[\Omega(t)]_{mn}[U^*(t)]_{n2} \\
&= \left([U(t)]_{22}\,[U(t)]_{23}\,[U(t)]_{25}\right) \begin{pmatrix} [\Omega(t)]_{22} & [\Omega(t)]_{23} & [\Omega(t)]_{25} \\ [\Omega(t)]_{32} & [\Omega(t)]_{33} & [\Omega(t)]_{35} \\ [\Omega(t)]_{52} & [\Omega(t)]_{53} & [\Omega(t)]_{55} \end{pmatrix} \begin{pmatrix} [\mathrm{U}^*(t)]_{22} \\ [\mathrm{U}^*(t)]_{32} \\ [\mathrm{U}^*(t)]_{52} \end{pmatrix} \\
&= \left([U(t)]_{22}\,[U(t)]_{23}\,[U(t)]_{25}\right) \widetilde{\Omega^{22}(t)} \begin{pmatrix} [\mathrm{U}^*(t)]_{22} \\ [\mathrm{U}^*(t)]_{32} \\ [\mathrm{U}^*(t)]_{52} \end{pmatrix}
\end{aligned} \tag{3.7}$$

The elements of $\widetilde{\Omega^{22}(t)}$ depend upon the initial state *i.e.*, the sets S1, S2, S3 and S4. It is difficult to understand the clear dependence of the population $[\rho^{123}(t)]_{22}$ in terms of the initial values of the matrix $\Omega(0)$ as they make up the population in a rather convoluted way according to (3.7). We give here a table with the values of $\Omega(0)$ for the different parameter sets S1-S4: The values of $\Omega(t)$ are obtained from the initial ones via relations $[\Omega(t)]_{kl} = [\Omega(t)]_{kl}e^{it\omega(k,l)}$ for a phases $\omega(k,l)$.

3.1.2 Entanglement measurement

In the present section we analyze the concurrence between spins i and j, as given in (2.84) and for the parameter values given by S1-S4, (3.4).

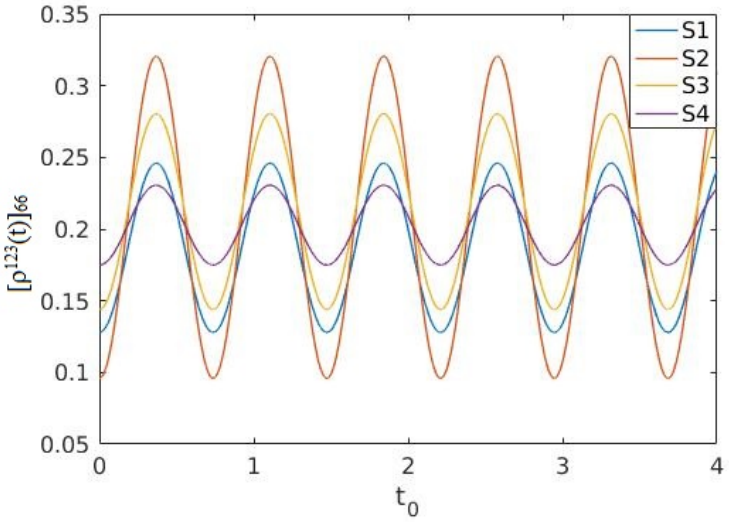

Figure 3.5: The diagonal element $[\rho^{123}(t)]_{66}$ as a function of the scaling time t_0 for the S_j in (3.4)

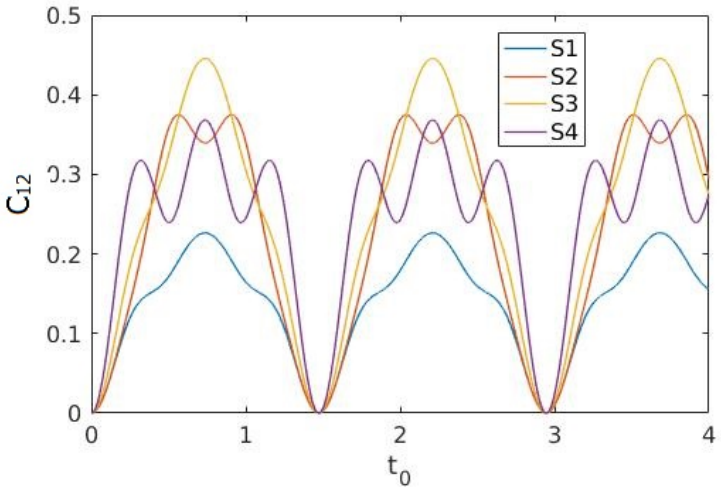

Figure 3.6: The concurrence C_{12} as a function of the scaling time t_0 for the S_j in (3.4)

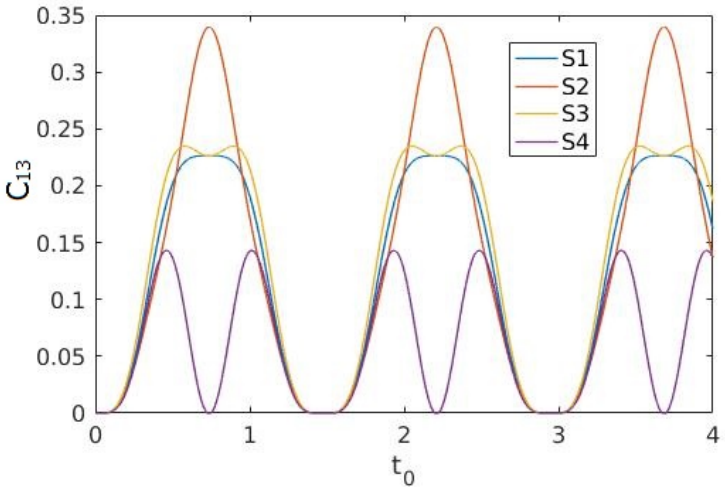

Figure 3.7: The concurrence C_{13} as a function of the scaling time t_0 for the S_j in (3.4)

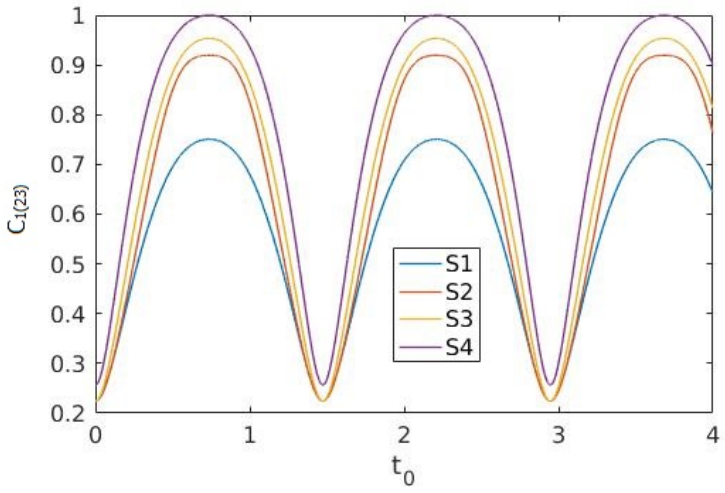

Figure 3.8: The concurrence $C_{1(23)}$ as a function of the scaling time t_0 for the S_j in (3.4)

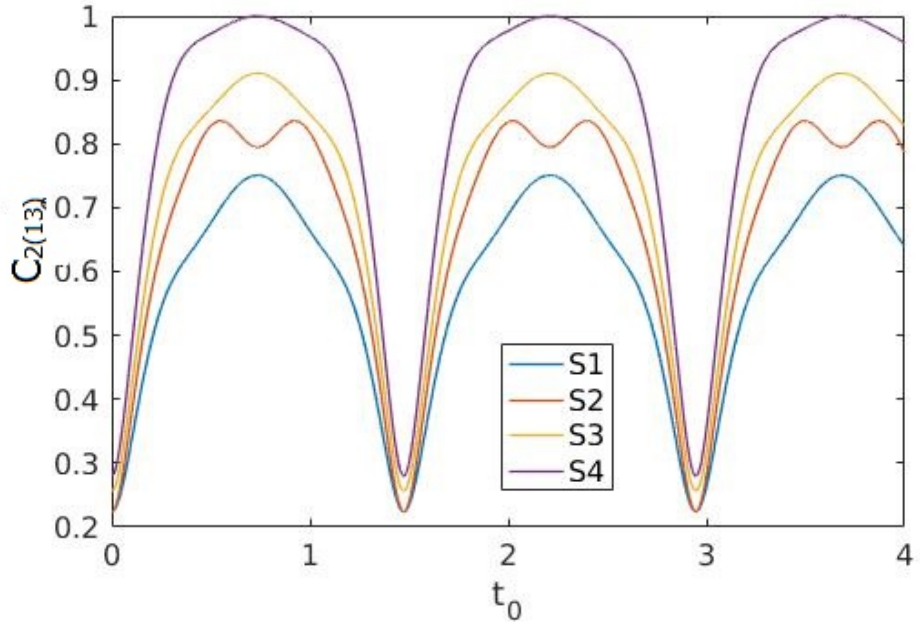

Figure 3.9: The concurrence $C_{2(13)}$ as a function of the scaling time t_0 for the S_j in (3.4)

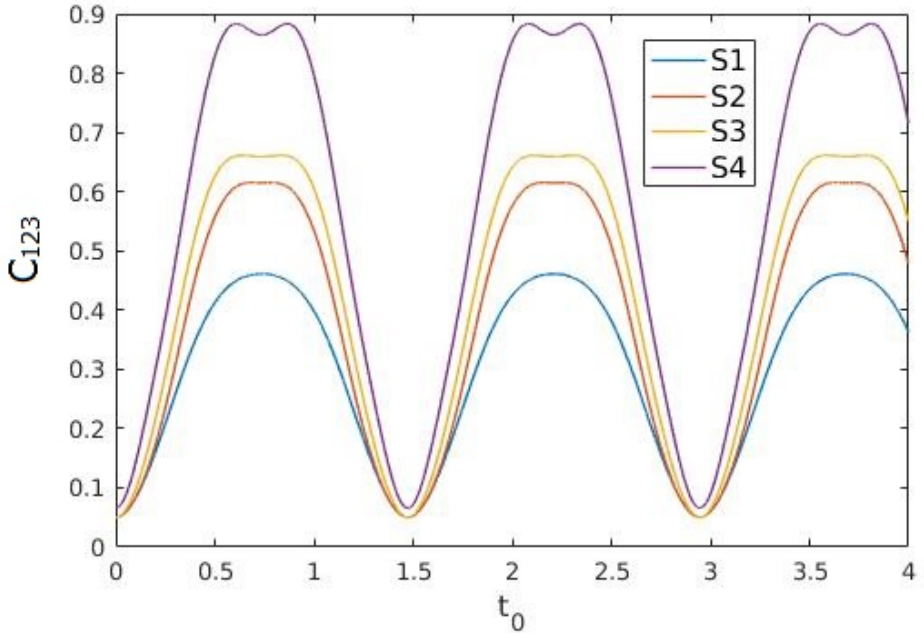

Figure 3.10: The concurrence C_{123} as a function of the scaling time t_0 for the S_j in (3.4)

	S1	S2	S3	S4
$[\Omega(0)]_{22}$	0.032	0.024	0.036	0.075
$[\Omega(0)]_{33}$	0.032	0.064	0.056	0.075
$[\Omega(0)]_{55}$	0.032	0.064	0.096	0.175
$[\Omega(0)]_{44}$	0.128	0.096	0.084	0.075
$[\Omega(0)]_{66}$	0.128	0.096	0.144	0.175
$[\Omega(0)]_{77}$	0.128	0.256	0.212	0.150

Table 3.1: The values of $[\Omega(0)]_{kk}$, $k = 2,3,5,4,6$ and 7 for the sets S1, S2, S3 and S4.

- The concurrence between spins 1 and 2, C_{12}, is presented in Figure 3.5. While the maximum values and times when they are reached, depend on the chosen parameters among S1-S4, the minimum values of C_{12} is zero for all of them, and the minimum is reached at times common for all parameter sets. All the four curves, the diagram of C_{12} are periodic with the same period. The maximum value of C_{12} for S3 is the biggest, and that of for S1 is the smallest. The maximum values of C_{12} for S2 and S4 are very close, and the maximum value of C_{12} for S1 is almost the half of the maximum value of C_{12} for S3. The curves C_{12} for S2 and S4 have more wavy nature compared to that of for S1 and S3.
- C_{13}, the concurrence between spins 1 and 3, is presented in Figure 3.6. We observe that the maximum values of C_{13} are 'not in sync' for the different sets S1-S4 (while they were in the previous case, for the adjacent spins 1 and 2). Nevertheless, the minimum values of C_{12} are the same (zero) for the four sets and occur at the same times. The C_{13} curves for four different sets, are periodic with the same period, but the periodicity of C_{13} curve for S4 is twice that of the others. The maximum value of C_{13} for S2 is the biggest, and that of for S4 is the smallest. The maximum values of C_{13} for S1 and S3 are very close, and the maximum value of C_{13} for S4 is less than the half of the maximum value of C_{13} for S2. The C_{13} curves for S3 has little bit more wavy nature compare to others.
- Figure 3.7 shows the concurrence between spin 1 and rest of the system: spins 2 and 3, $C_{1(23)}$ (see (2.89)). All the four curves are periodic with the same period and monotonic for all times (S4 always the largest). It follows from the figure that the maximum values of $C_{1(23)}$ are different for the Sj but again, the minimum values of $C_{1(23)}$ is almost the same for the four sets and they occur at the same time. Contrary to the two-spin entanglement of the previous case, here *the minimal entanglement is not vanishing*. There is generally *much more* entanglement between one spin and the other two, than just between two of them. The maximum value of $C_{1(23)}$ for S4 is the biggest which is exactly one, and that of for S1 is the smallest.
- Figure 3.8 shows the concurrence between spin 2 and rest of the system: spins 1 and 3, $C_{2(13)}$ (see (2.89)). All the four curves are periodic with the same period. It follows from the figure that the maximum values of $C_{2(13)}$ depend on the set S1-S4 are different. The minima are achieved at the same moments in time for all parameter regimes, and again, the minimal concurrence is strictly positive. The maximum value of $C_{2(13)}$ for S4 is the biggest which is exactly one, and that of for S1 is the smallest.
- Figure 3.9 shows the intrinsic three-spin entanglement, C_{123} (see (2.90)). All the four curves are periodic with the same period. It follows from the figure that the maximum values of C_{123} for four different sets S1, S2, S3, S4 are different; although, the minimum values of C_{123} are almost the same for the four sets and occur at the same times. The maximum value of C_{123} for S4 is the biggest, and that of for S1 is the smallest.

3.2 Dynamics of the chain coupled to a single reservoir

In the previous section we already discussed the population and entanglement for the system of a linear spin chain of three spins not coupled to any reservoir. Now we are going to analyze the concurrence for a three spin chain interacting with a single reservoir. We consider merely the presence of one (the lower) reservoir $R_L(\lambda_L, T_L)$, as sketched in Figure 3.11.

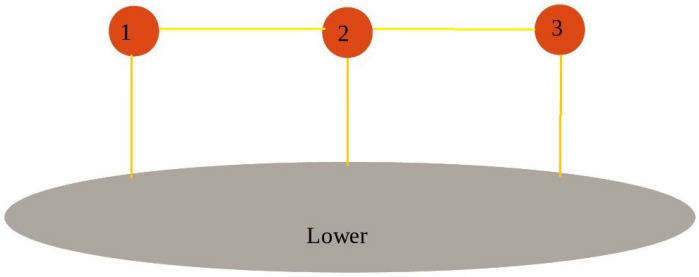

Figure 3.11: A schematic representation of the present system. The spin chain of the three spins 1, 2 and 3 is connected to a single bosonic reservoir, the 'Lower (L)' reservoir.

3.2.1 Fixed temperature and varying coupling parameter, Figures 3.12-3.16

In the present scenario we consider different values for reservoir coupling parameter λ_L and a fixed reservoir temperature $T_L = 100K$. We consider the initial spin chain in the state characterized by $p_1 = 0.2$, $p_2 = 0.3$ $p_3 = 0.4$ and the off diagonals v_j as in (3.3). This corresponds to S3 in (3.4).

- The concurrence between spins 1 and 2, C_{12}, is presented in Figure 3.12, for four values of the reservoir coupling parameter λ_L. Without coupling to the reservoir ($\lambda_L = 0$), the concurrence C_{12} is oscillating uniformly in a wide region $[0, 0.445]$. When the interaction with the reservoir is turned on ($\lambda_L \neq 0$), then the concurrence traverses a intermediate (not periodic) phase and reaches a 'stationary' oscillating regime after a characteristic time. The characteristic 'relaxation' time to reach the steady regime depends on the strength of the coupling λ_L. The weaker the coupling constant (λ_L smaller) the larger the relaxation time. This is physically to be expected, as the relaxation is an effect induced by the reservoir! In the stationary regime, the concurrence C_{12} is confined to the much smaller range $[0.06, 0.17]$, another reservoir effect. We note that in the steady regime, the concurrence C_{12} is strictly positive at all times, i.e., spins 1 and 2 are continuously entangled. This is in contrast to the dynamics without coupling to the reservoir, where the concurrence vanishes periodically.
- The concurrence between spins 1 and 3, C_{13}, is presented in Figure 3.13. The amplitude of C_{13} is oscillating uniformly in a wide region $[0, 0.23]$ for $\lambda_L = 0$. As for the concurrence of spins 1 and 2, a steady (oscillating) regime is reached after a characteristic relaxation time which increases as λ_L decreases. The difference is that in that steady regime, the concurrence *does* vanish periodically. The reservoir 'does not manage' to entangle the non-nearest neighbour spins 1 and 3 at all times. Moreover, the maximal entanglement between spins 1 and 3 is less than half of that between 1 and 2.
- Figure 3.14 shows the concurrence between spin 1 and rest of the system: spins 2 and 3, $C_{1(23)}$. For $\lambda_L = 0$, $C_{1(23)}$ is oscillating uniformly in a wide region $[0.23, 0.95]$. Again, the concurrence enters a oscillating stationary regime after a characteristic relaxation time (which grows as λ_L shrinks). However, now, the effect of the reservoir is to create *a lot of concurrence*. Namely, $C_{1(23)}$ oscillates within $[0.8, 0.98]$. $C_{1(23)}$ takes longer time to reach in

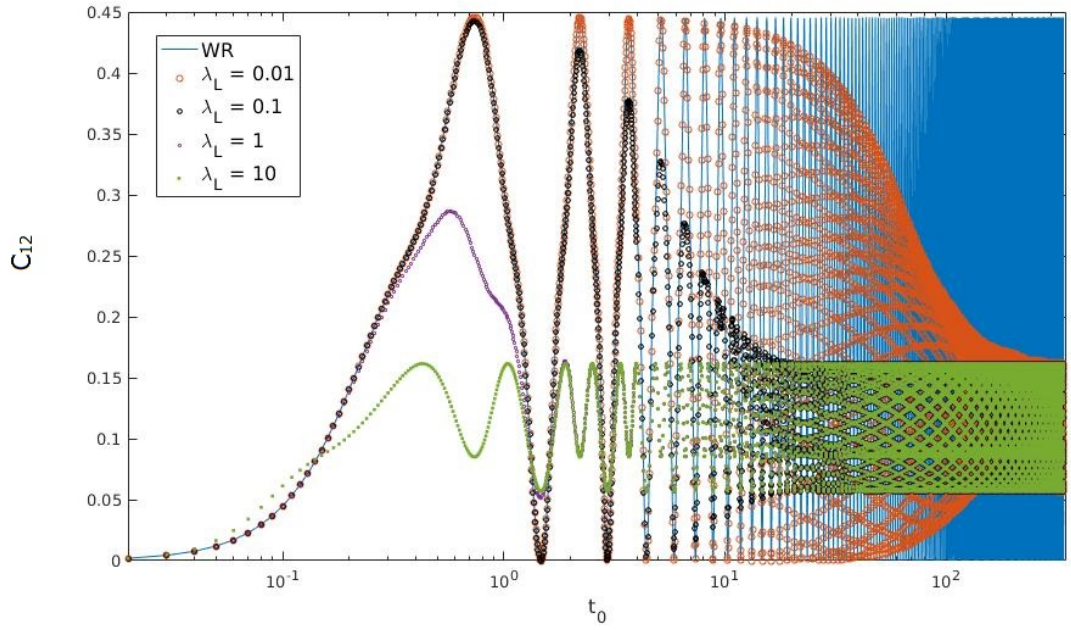

Figure 3.12: The concurrence C_{12} as a function of the scaling time t_0 for $p_1 = 0.2$, $p_2 = 0.3$, $p_3 = 0.4$ and fixed reservoir temperature $T_L = 100K$. Note that the time is reported on a log-scale. Here we consider several values of the reservoir coupling parameter λ_L as indicated within the figure. The blue curve, WR, shows the concurrence C_{12} without reservoir coupling ($\lambda_L = 0$). It coincides with the curve for S3 in Figure 3.6.

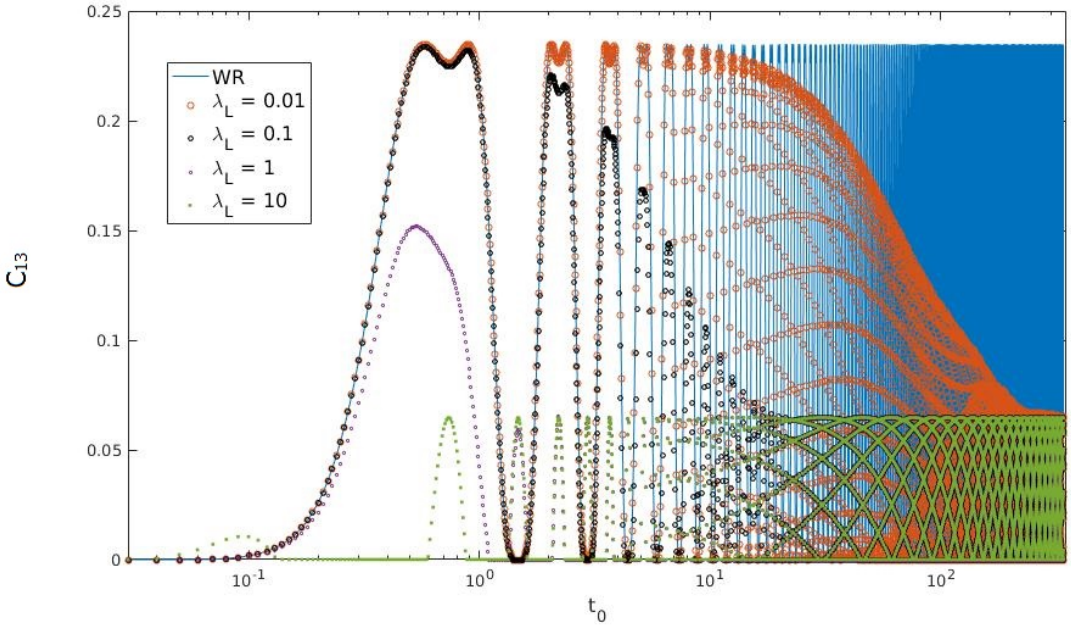

Figure 3.13: The concurrence C_{13} as a function of the scaling time t_0 for $p_1 = 0.2$, $p_2 = 0.3$, $p_3 = 0.4$ and fixed reservoir temperature $T_L = 100K$. Here we consider several values of the reservoir coupling parameter λ_L as indicated in figure, and WR denotes the concurrence C_{13} for $\lambda_L = 0$.

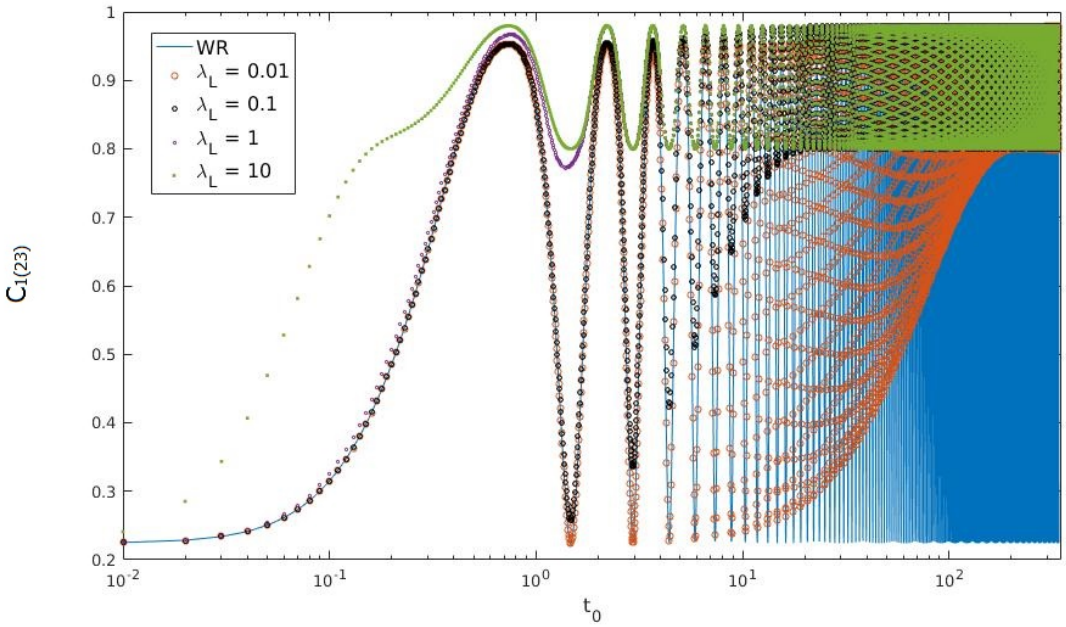

Figure 3.14: The concurrence $C_{1(23)}$ as a function of the scaling time t_0 for $p_1 = 0.2$, $p_2 = 0.3$, $p_3 = 0.4$ and fixed reservoir temperature $T_L = 100$K. Here we consider several values of reservoir coupling parameter λ_L as indicated in figure, and WR denotes the concurrence $C_{1(23)}$ for $\lambda_L = 0$.

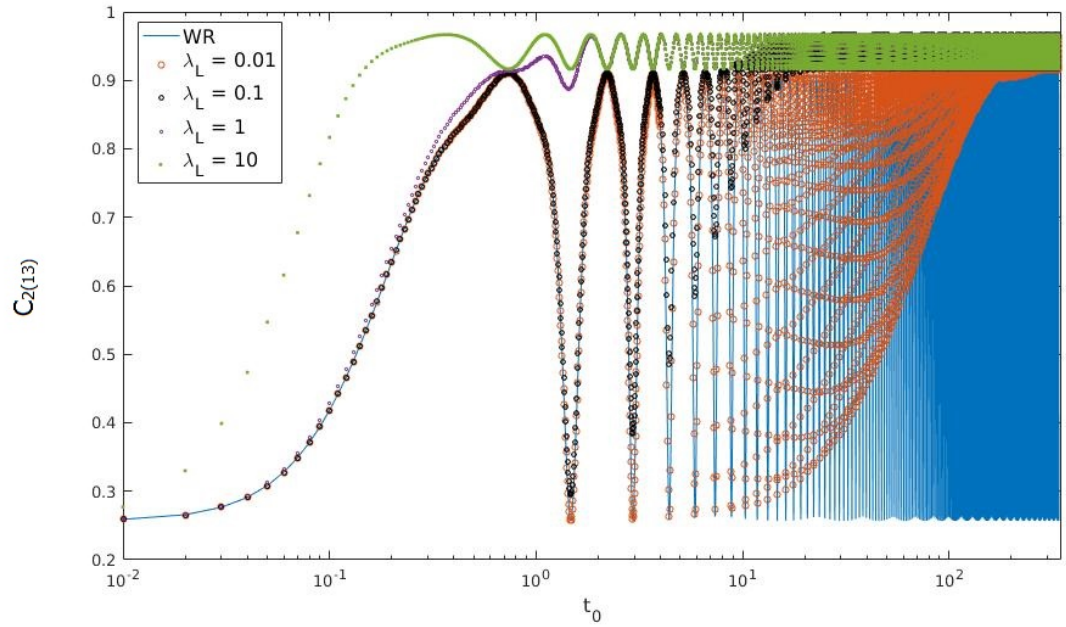

Figure 3.15: The concurrence $C_{2(13)}$ as a function of the scaling time t_0 for $p_1 = 0.2$, $p_2 = 0.3$, $p_3 = 0.4$ and fixed reservoir temperature $T_L = 100$K. Here we consider several values of reservoir coupling parameter λ_L as indicated in figure, and WR denotes the concurrence $C_{2(13)}$ for $\lambda_L = 0$.

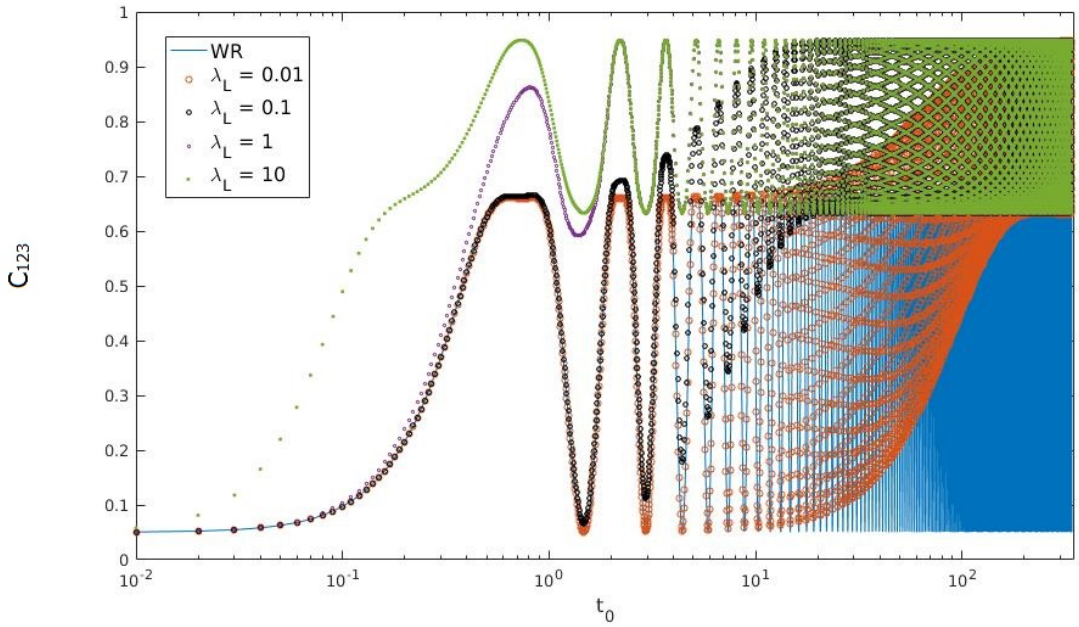

Figure 3.16: The concurrence C_{123} as a function of the scaling time t_0 for $p_1 = 0.2$, $p_2 = 0.3$, $p_3 = 0.4$ and fixed reservoir temperature $T_L = 100K$. Here we consider several values of reservoir coupling parameter λ_L as indicated in figure, and WR denotes the concurrence C_{123} for $\lambda_L = 0$.

the steady state when the reservoir coupling parameter λ_L is comparatively low. Figure 3.14 shows that the maximum value of $C_{1(23)}$ as $\lambda_L \neq 0$ is *larger* than that of the blue WR curve (which corresponds to $\lambda_L = 0$), while the minimum value is significantly higher than that of WR.

- Figure 3.15 shows the concurrence between spin 2 and rest of the system: spins 1 and 3, $C_{2(13)}$. For $\lambda_L - 0$, $C_{2(13)}$ oscillates within $[0.23, 0.91]$. This concurrence is qualitatively similar to $C_{1(23)}$ with the difference that the amplitude of oscillation is located within $[0.91, 0.98]$, a narrower band located closer to the maximum value 1. We also discover that the *minimal* value of $C_{2(13)}$ for $\lambda_L \neq 0$ equals the *maximal* one for the case $\lambda_L = 0$.
- Figure 3.16 shows the intrinsic three-spin entanglement, C_{123}, which for $\lambda_L = 0$ oscillates uniformly in a wide region $[0.08, 0.66]$. The steady regime shows oscillations in $[0.62, 0.95]$, which is much wider than for $C_{2(13)}$.

3.2.2 Fixed coupling parameter and varying temperature, Figures 3.17-3.21

In the present section, we vary the reservoir temperature T_L while $\lambda_L = 0.01$ is fixed. In addition for the initial state, we consider $p_1 = 0.2$, $p_2 = 0.3$, $p_3 = 0.5$, which is S3 in (3.4).

- The concurrence between spins 1 and 2, C_{12}, is presented in Figure 3.17 for different values of the reservoir temperature T_L. For $\lambda_L = 0$, C_{12} is oscillating in the region $[0, 0.445]$. The coupling with the reservoir drives the concurrence to steady regime, oscillating within the values $[0.06, 0.17]$. We see that the characteristic time scale for C_{12} to reach its steady regime increases as the temperature increases. This is physically plausible, since a hotter reservoir will speed up the reservoir effect induced on the system dynamics. For $t_0 < 1$, the values of C_{12} for $T_L = 100K$ and $200K$ coincide with the values of C_{12} with $\lambda_L = 0$. The figure shows that due to the reservoir coupling, in the steady regime, $C_{12} \geq 0.06$ is always nonzero. So spins 1 and 2 are continuously entangled. However, the maximum value of C_{12} is reduced

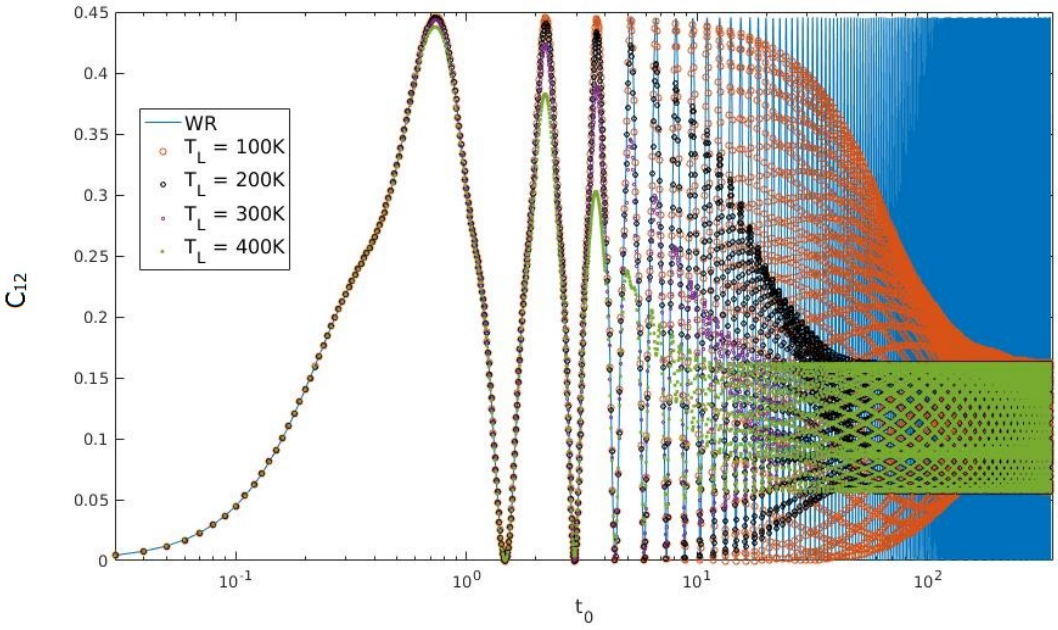

Figure 3.17: The concurrence C_{12} as a function of the scaling time t_0 for $p_1 = 0.2$, $p_2 = 0.3$, $p_3 = 0.4$ and fixed reservoir coupling parameter $\lambda_L = 0.01$. Here we consider several values of reservoir temperature T_L as indicated in figure, and WR denotes the concurrence C_{12} for $\lambda_L = 0$.

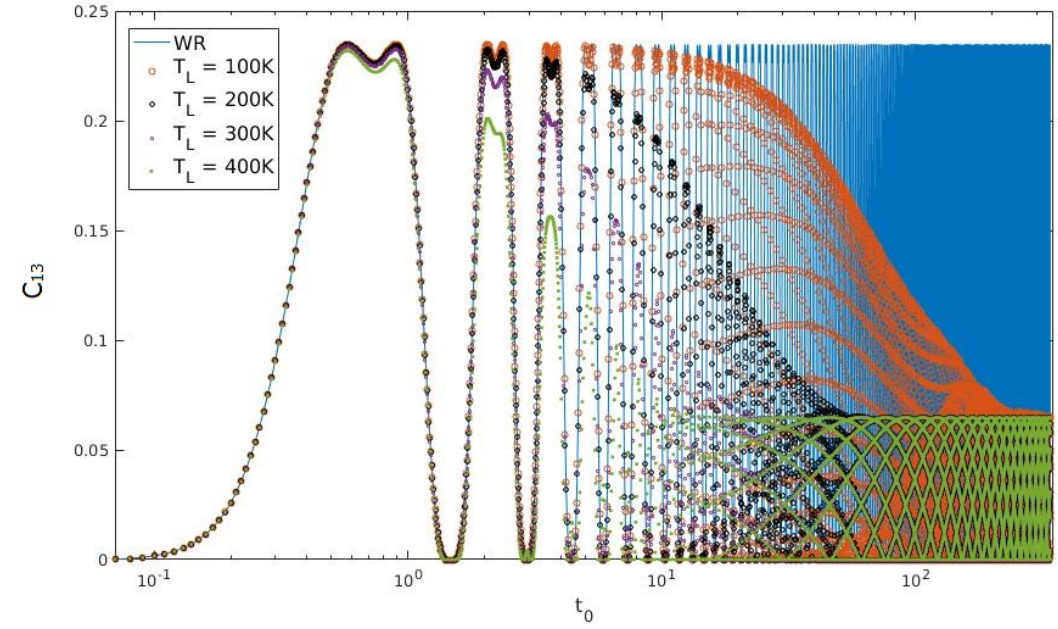

Figure 3.18: The concurrence C_{13} as a function of the scaling time t_0 for $p_1 = 0.2$, $p_2 = 0.3$, $p_3 = 0.4$ and fixed reservoir coupling parameter $\lambda_L = 0.01$. Here we consider several values of reservoir temperature T_L as indicated in figure, and WR denotes the concurrence C_{13} for $\lambda_L = 0$.

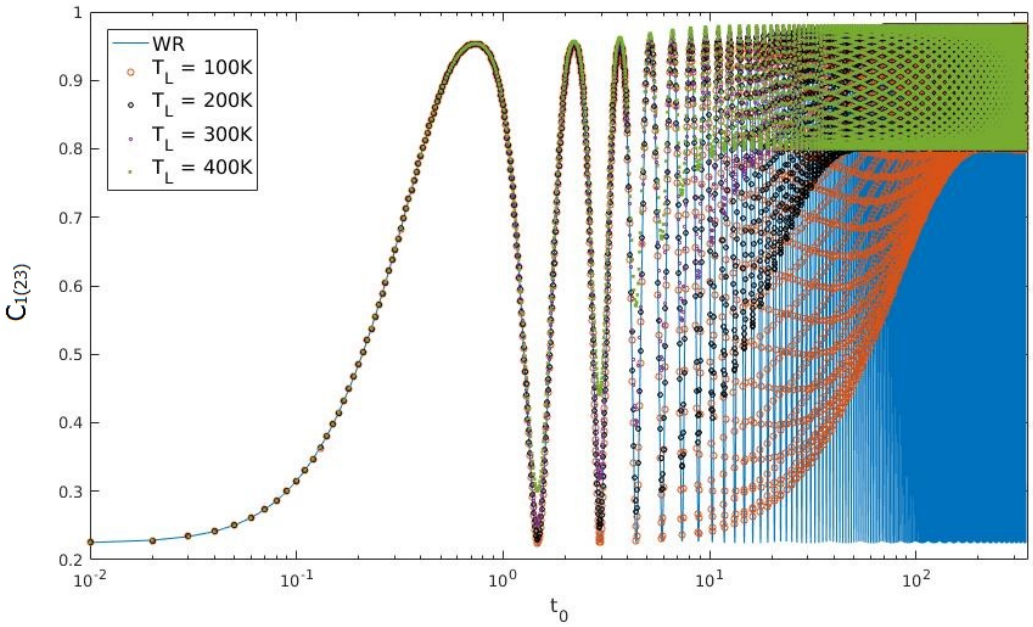

Figure 3.19: The concurrence $C_{1(23)}$ as a function of the scaling time t_0 for $p_1 = 0.2$, $p_2 = 0.3$, $p_3 = 0.4$ and fixed reservoir coupling parameter $\lambda_L = 0.01$. Here we consider several values of reservoir temperature T_L as indicated in figure, and WR denotes the concurrence $C_{1(23)}$ for $\lambda_L = 0$.

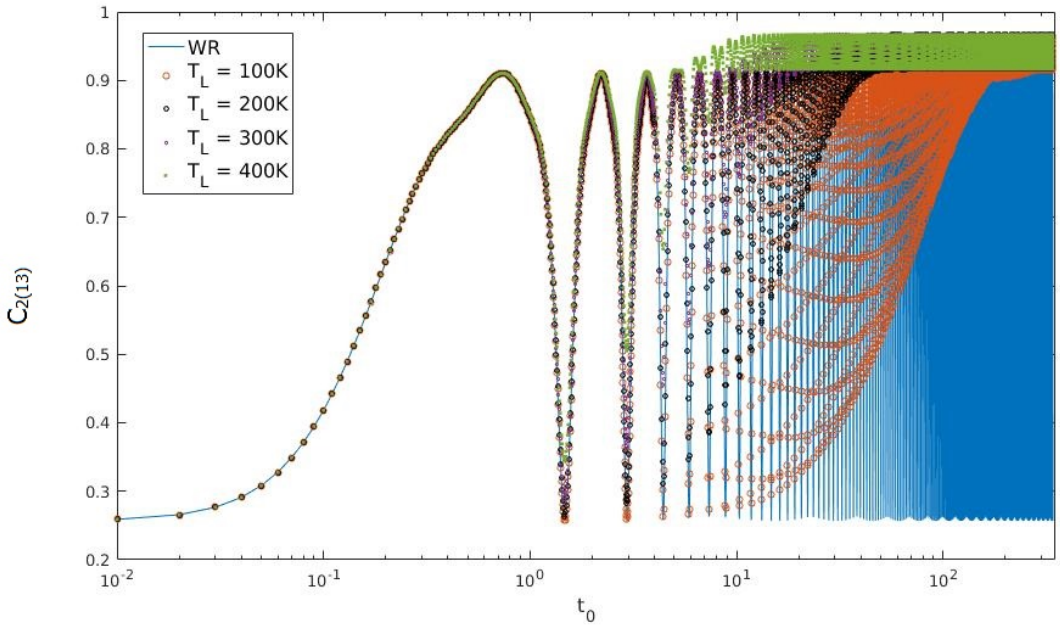

Figure 3.20: The concurrence $C_{2(13)}$ as a function of the scaling time t_0 for $p_1 = 0.2$, $p_2 = 0.3$, $p_3 = 0.4$ and fixed reservoir coupling parameter $\lambda_L = 0.01$. Here we consider several values of reservoir temperature T_L as indicated in figure, and WR denotes the concurrence $C_{2(13)}$for $\lambda_L = 0$.

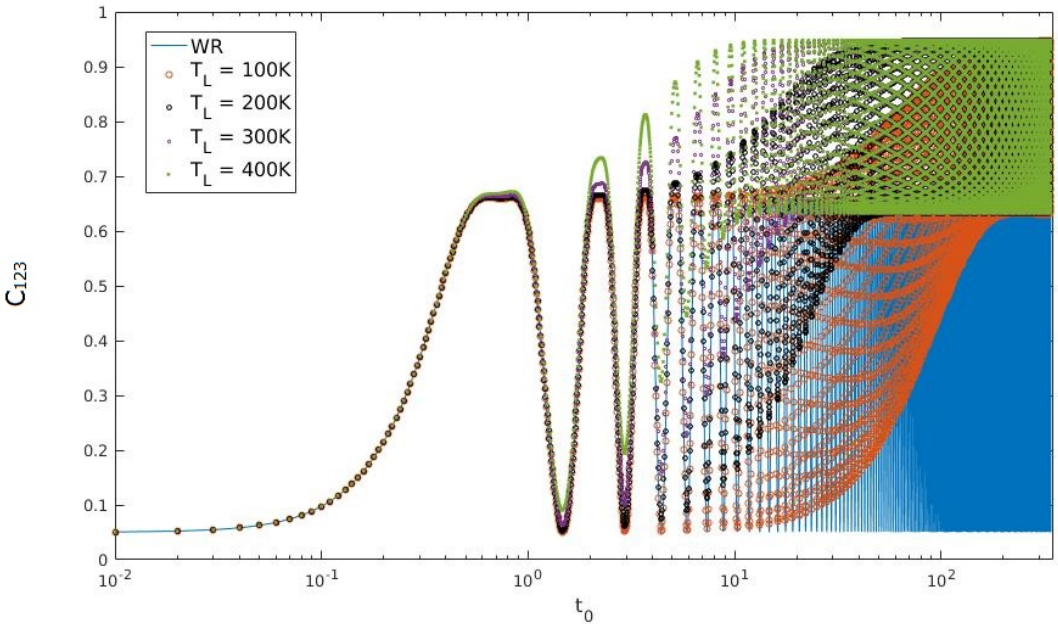

Figure 3.21: The concurrence C_{123} as a function of the scaling time t_0 for $p_1 = 0.2$, $p_2 = 0.3$, $p_3 = 0.4$ and fixed reservoir coupling parameter $\lambda_L = 0.01$. Here we consider several values of reservoir temperature T_L as indicated in figure, and WR denotes the concurrence $C_{123}$for $\lambda_L = 0$.

due to reservoir effect, as compared to the case $\lambda_L = 0$.

- The concurrence between spins 1 and 3, C_{13}, is presented in Figure 3.18 for different values of reservoir temperature T_L. For $\lambda_L = 0$, C_{13} is oscillating in the region $[0, 0.23]$. The coupling with the reservoir drives the concurrence to steady regime, oscillating within the values $[0, 0.07]$ and the relaxation time to reach the steady regime is again decreasing as T_L increases. The difference with the concurrence C_{12} is that spins 1 and 3 are *less* entangled than the neighbouring spins 1 and 2. And indeed, there are periodic moments in time where $C_{13} = 0$. For $t_0 < 1$, the values of C_{13} for $T_L = 100K$ and $200K$ again coincide with those for $\lambda_L = 0$.
- Figure 3.19 shows the concurrence between spin 1 and rest of the system: spins 2 and 3, $C_{1(23)}$ as a function of T_L. Again, a steady regime is reached as in the previous cases, the difference being now that the value of this concurrence can be very large, close to the maximum possible, $C_{1(23)} = 1$.
- Figure 3.20 shows the concurrence between spin 2 and rest of the system: spins 1 and 3, $C_{2(13)}$. The only quantitative real difference with $C_{1(23)}$ is that the oscillations in the stationary regime has a much smaller amplitude, about $1/4$ that of $C_{1(23)}$.
- Figure 3.21 shows the intrinsic three-spin entanglement, C_{123}. For $\lambda_L = 0$, C_{123} oscillates in $[0.08, 0.66]$. In the steady regime for $\lambda_L \neq 0$, this range is $[0.62, 0.95]$.

3.3 Dynamics of the chain coupled to two reservoirs

In the previous section, we analyzed the concurrences in the spin chain coupled to a single reservoir. Now we consider the case of two reservoirs $R_L(\lambda_L, T_L)$ and $R_U(\lambda_U, T_U)$, as sketched in Figure 3.22.

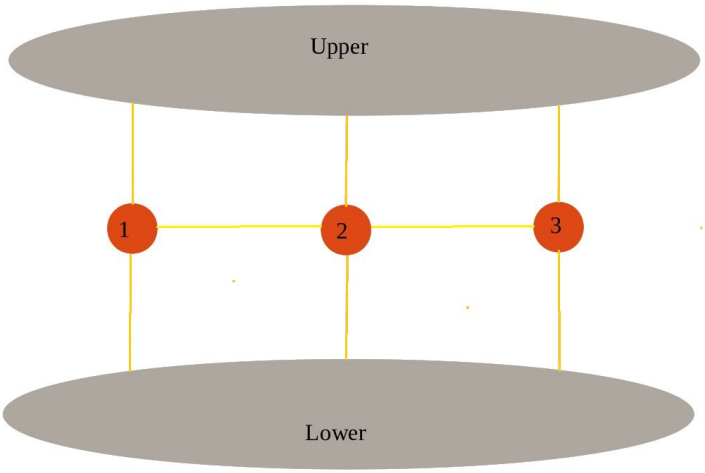

Figure 3.22: A schematic representation of the present system. The spin chain connected to two bosonic reservoirs, labelled by 'Lower (L)' and 'Upper (U)', respectively.

Here we consider two different values of the reservoir coupling parameters, and the temperature difference of two reservoirs is fixed to be $100K$. We consider two separate cases

- *Case I* $\lambda_L = \lambda_U = 0.01$, $|T_L - T_U| = 100K$, Section 3.3.1
- *Case II* $\lambda_L = \lambda_U = 0.1$, $|T_L - T_U| = 100K$, Section 3.3.2

In the following sections, we compare the values of the concurrences for the two reservoirs system with those of for the single reservoir system. For the single reservoir system, we take λ_L = 0.01 and $T_L = 100K$ for the case I, while we take $\lambda_L = 0.1$ and $T_L = 100K$ for the case II.

3.3.1 Case I: $\lambda_L = \lambda_U = 0.01$ and $|T_L - T_U| = 100K$, Figures 3.23-3.27

The initial condition is given by $p_1 = 0.3$, $p_2 = 0.5$, $p_3 = 0.5$, see (2.9) and (3.3).

- Figure 3.23 shows the concurrence between spins 1 and 2, C_{12}, for ($T_L = 100K$, $T_U = 200K$) and ($T_L = 200K$, $T_U = 300K$). We compare C_{12} of the double reservoirs system with C_{12} of single reservoir system with $\lambda_L = 0.01$ and $T_L = 100K$. We observe that for all three curves, the maximum and the minimum values of C_{12} are 0.37 and 0, respectively. Also, in the steady regime all three curves oscillate between the same values 0.22 and 0.08. At fixed $|T_L - T_U|$, the relaxation to the steady regime happens quicker when T_L is increased, which is physically correct. The steady regime is also reached quicker in the double-reservoir situation as compared to the single reservoir one. Moreover, we checked numerically that as $|T_L - T_U|$ is increased, at fixed T_L, the process is quicker. Again, this is physically correct, as a bigger temperature gradient will accelerate the relaxation process.
- Figure 3.24 shows that the concurrence between spins 1 and 2, C_{13}. As in the previous discussion, the general feature here is that less entanglement is created between the distant spins 1 and 3, as compared to spins 1 and 2 (Fig. 3.23). There are moment in, time, periodically, when the concurrence vanishes.
- Figure 3.25 and 3.26 show the concurrences between spins 1 and (2,3) and spins 2 and (1,3), respectively. We observe the by now expected behaviour: high values of entanglement

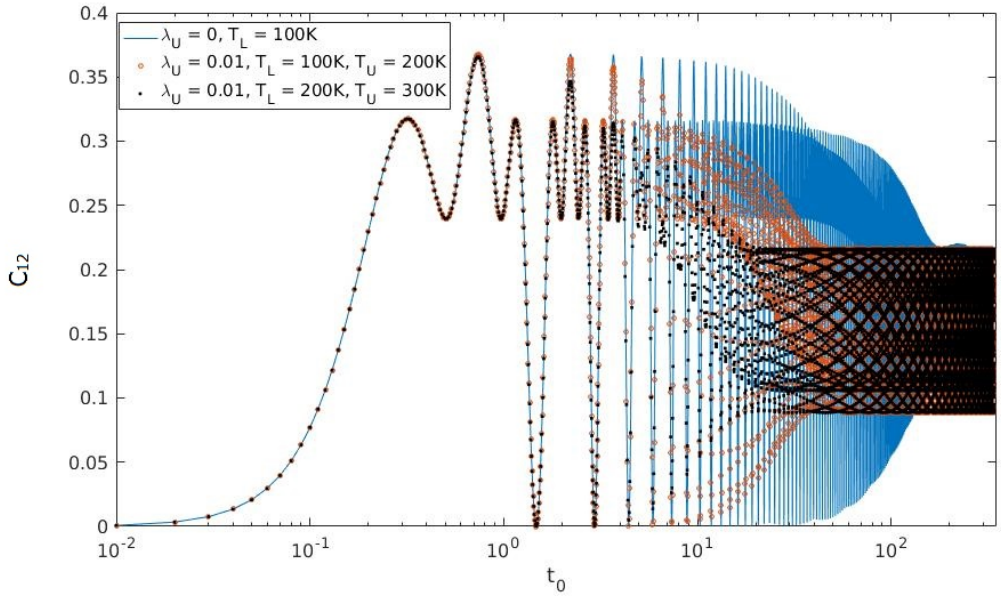

Figure 3.23: The concurrence C_{12} as a function of the scaling time t_0 for $p_1 = 0.3$, $p_2 = 0.5$, $p_3 = 0.5$ and fixed reservoir coupling parameter $\lambda_L = 0.01$ for single reservoir (blue curve) as well as double reservoirs. $\lambda_U = 0$ indicates the system of single reservoir, and $\lambda_U = 0.01$ indicates the system of double reservoirs. Here we consider the temperature of the single reservoir system, $T_L = 100K$, and the temperature difference of the double reservoir system, $|T_L - T_R| = 100K$. For the double reservoirs case we consider two different sets of values of (T_L, T_R).

are created in the stationary regime, with a minimal amount of entanglement ≈ 0.9. The difference in the two figures is the width of the oscillation band in the stationary regime.

- Figure 3.27 shows the intrinsic concurrence C_{123}. High values are achieved in the stationary regime, with a minimum value of ~ 0.8.

3.3.2 Case II: $\lambda_L = \lambda_U = 0.1$ and $|T_L - T_U| = 100K$, Figures 3.28-3.32

We now consider an increase by a factor 10 of the coupling constants relative to Section 3.3.1, $\lambda_L = \lambda_U = 0.1$. The initial state is as before, $p_1 = 0.3$, $p_2 = 0.5$, $p_3 = 0.5$.

The graphs in the following figures are qualitatively *the same* as the ones in case I, Section 3.3.1, with the only modification that the stationary regime is reached more quickly here. This is simply due to the fact that we have now increased the coupling strength of the system-reservoir interaction. We present the figures with captions but no further discussion.

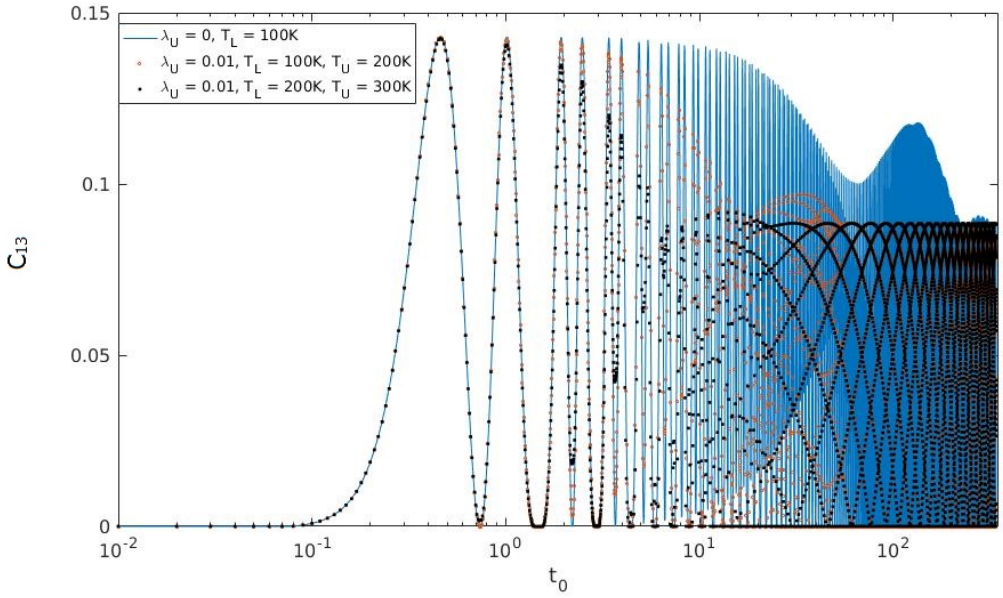

Figure 3.24: The concurrence C_{13} as a function of the scaling time t_0 for $p_1 = 0.3$, $p_2 = 0.5$, $p_3 = 0.5$ and fixed reservoir coupling parameter $\lambda_L = 0.01$ for single reservoir as well as double reservoirs. $\lambda_U = 0$ indicates the system of single reservoir, and $\lambda_U = 0.01$ indicates the system of double reservoirs. Here we consider the temperature of the single reservoir system, T_L, is 100K, and the temperature difference of the double reservoir system, $T_L \sim T_R$, is 100K. For double reservoirs case we consider two different sets of values of (T_L, T_R).

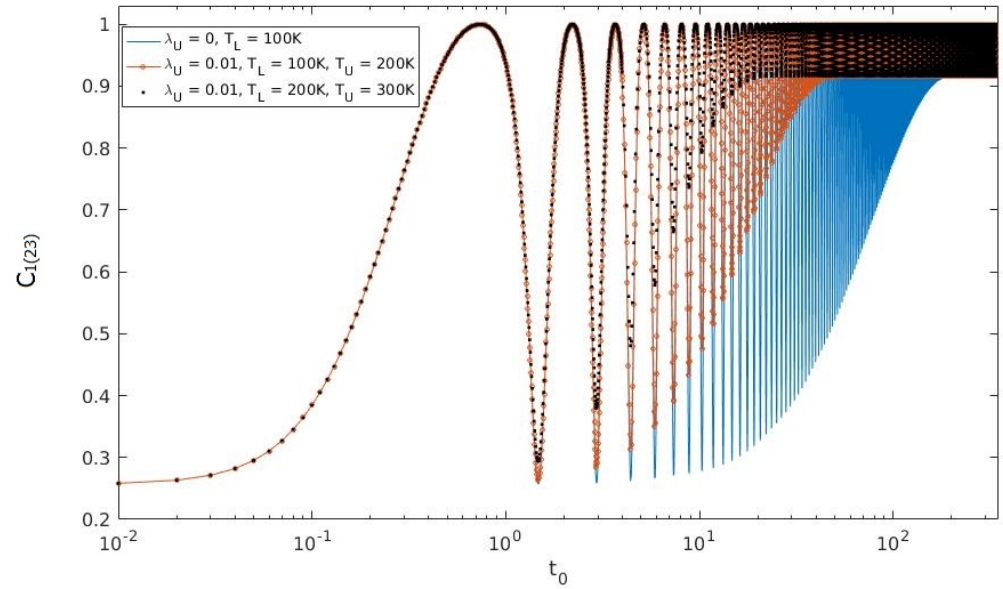

Figure 3.25: The concurrence $C_{1(23)}$ as a function of the scaling time t_0 for $p_1 = 0.3$, $p_2 = 0.5$, $p_3 = 0.5$ and fixed reservoir coupling parameter $\lambda_L = 0.01$ for single reservoir as well as double reservoirs. $\lambda_U = 0$ indicates the system of single reservoir, and $\lambda_U = 0.01$ indicates the system of double reservoirs. Here we consider the temperature of the single reservoir system, T_L, is 100K, and the temperature difference of the double reservoir system, $T_L \sim T_R$, is 100K. For double reservoirs case we consider two different sets of values of (T_L, T_R).

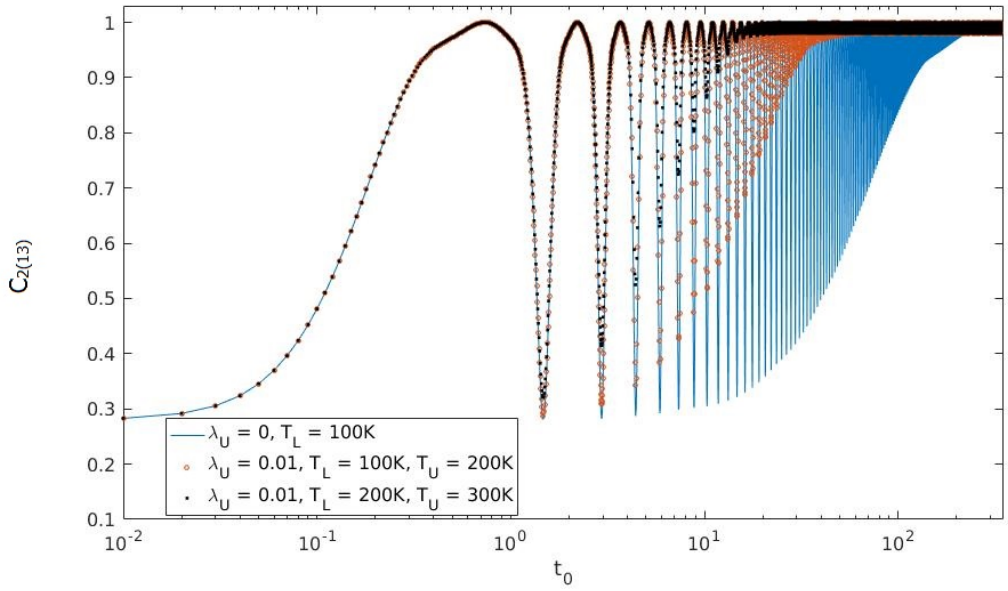

Figure 3.26: The concurrence $C_{2(13)}$ as a function of the scaling time t_0 for $p_1 = 0.3$, $p_2 = 0.5$, $p_3 = 0.5$ and fixed reservoir coupling parameter $\lambda_L = 0.01$ for single reservoir as well as double reservoirs. $\lambda_U = 0$ indicates the system of single reservoir, and $\lambda_U = 0.01$ indicates the system of double reservoirs. Here we consider the temperature of the single reservoir system, T_L, is 100K, and the temperature difference of the double reservoir system, $T_L \sim T_R$, is 100K. For double reservoirs case we consider two different sets of values of (T_L, T_R).

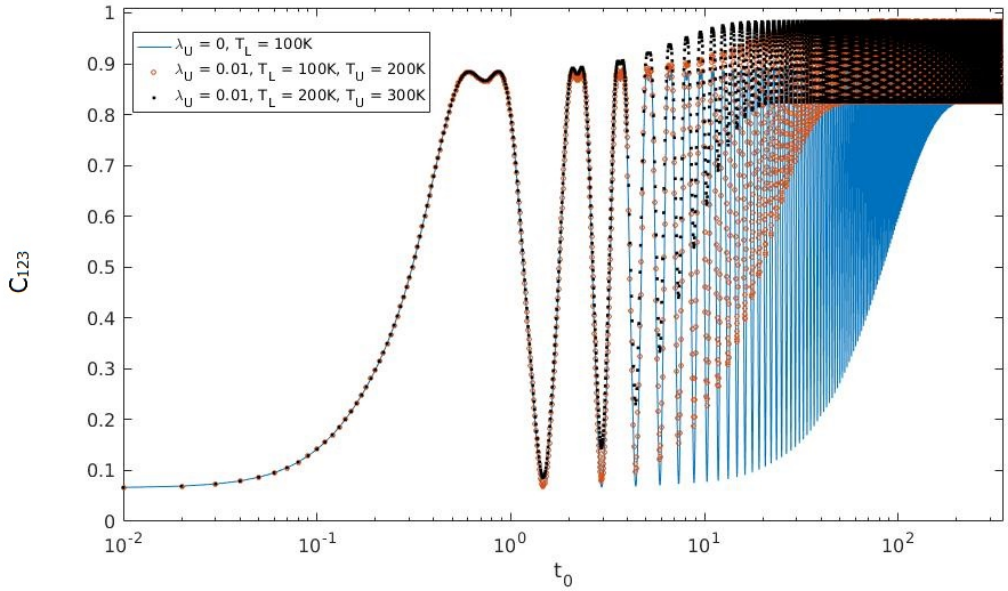

Figure 3.27: The concurrence C_{123} as a function of the scaling time t_0 for $p_1 = 0.3$, $p_2 = 0.5$, $p_3 = 0.5$ and fixed reservoir coupling parameter $\lambda_L = 0.01$ for single reservoir as well as double reservoirs. $\lambda_U = 0$ indicates the system of single reservoir, and $\lambda_U = 0.01$ indicates the system of double reservoirs. Here we consider the temperature of the single reservoir system, T_L, is 100K, and the temperature difference of the double reservoir system, $T_L \sim T_R$, is 100K. For double reservoirs case we consider two different sets of values of (T_L, T_R).

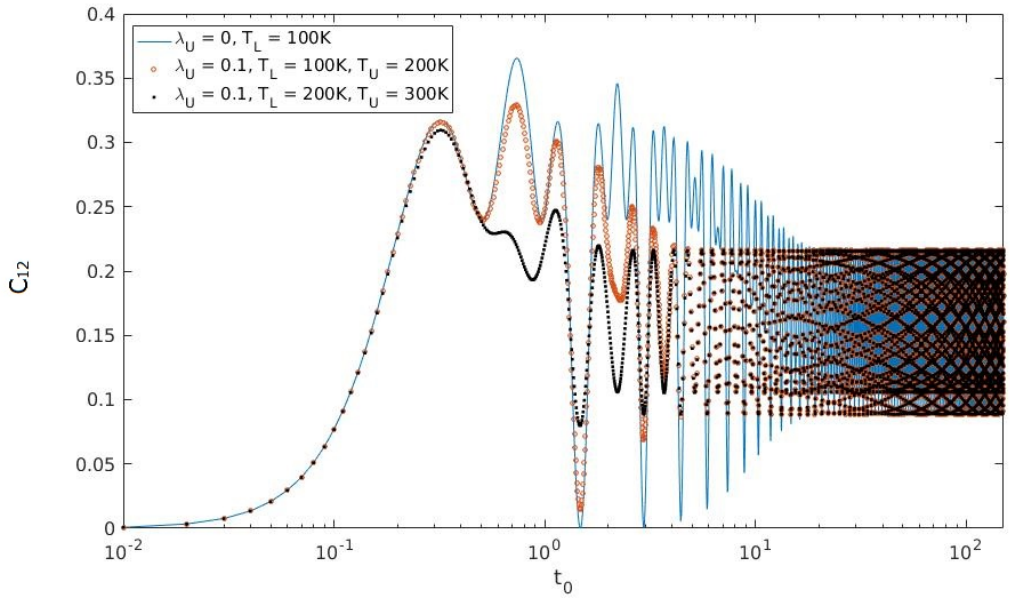

Figure 3.28: The concurrence C_{12} as a function of the scaling time t_0 for $p_1 = 0.3$, $p_2 = 0.5$, $p_3 = 0.5$ and fixed reservoir coupling parameter $\lambda_L = 0.1$ for a single reservoir as well as for double reservoirs. $\lambda_U = 0$ indicates the system of single reservoir, and $\lambda_U = 0.1$ indicates the system of double reservoirs. Here we consider the temperature of the single reservoir system, T_L, is 100K, and the temperature difference of the double reservoir system, $T_L \sim T_R$, is 100K. For double reservoirs case we consider two different sets of values of (T_L, T_R) as indicated in Figure.

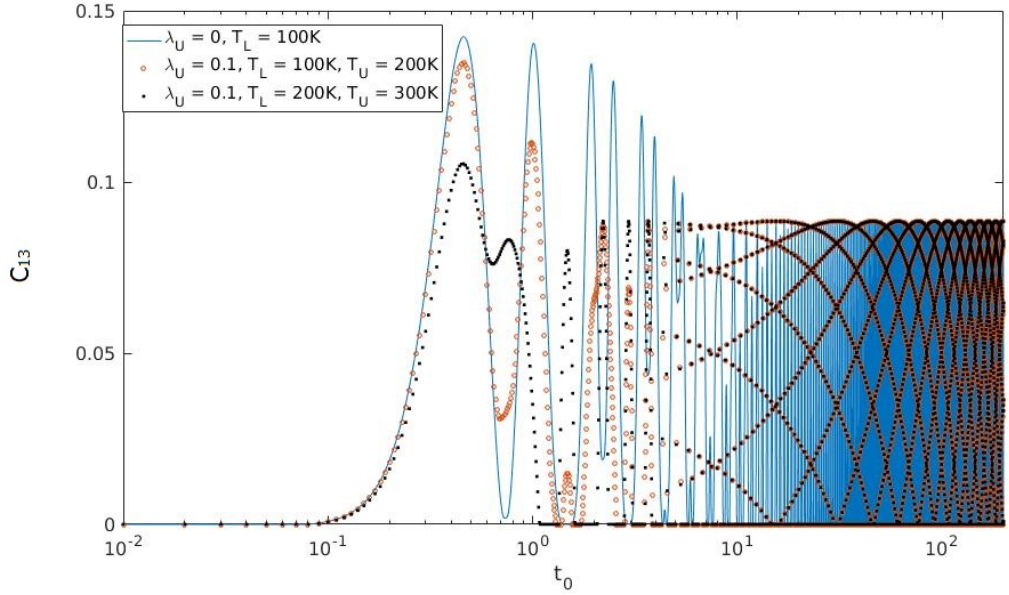

Figure 3.29: The concurrence C_{13} as a function of the scaling time t_0 for $p_1 = 0.3$, $p_2 = 0.5$, $p_3 = 0.5$ and fixed reservoir coupling parameter $\lambda_L = 0.1$ for a single reservoir as well as for double reservoirs. $\lambda_U = 0$ indicates the system of single reservoir, and $\lambda_U = 0.1$ indicates the system of double reservoirs. Here we consider the temperature of the single reservoir system, T_L, is 100K, and the temperature difference of the double reservoir system, $T_L \sim T_R$, is 100K. For double reservoirs case we consider two different sets of values of (T_L, T_R) as indicated in Figure.

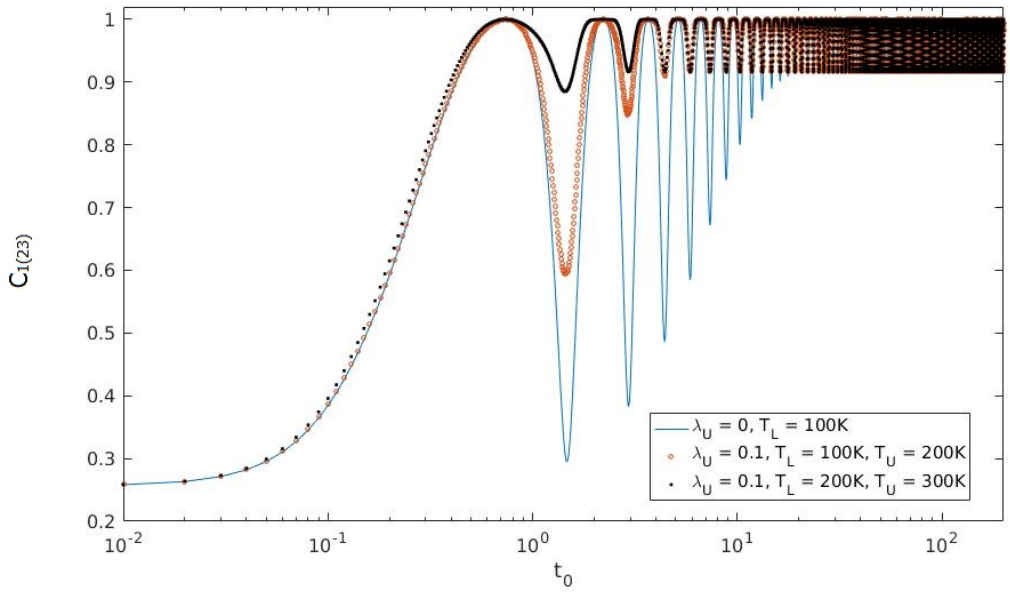

Figure 3.30: The concurrence $C_{1(23)}$ as a function of the scaling time t_0 for $p_1 = 0.3$, $p_2 = 0.5$, $p_3 = 0.5$ and fixed reservoir coupling parameter $\lambda_L = 0.1$ for a single reservoir as well as for double reservoirs. $\lambda_U = 0$ indicates the system of single reservoir, and $\lambda_U = 0.1$ indicates the system of double reservoirs. Here we consider the temperature of the single reservoir system, T_L, is 100K, and the temperature difference of the double reservoir system, $T_L \sim T_R$, is 100K. For double reservoirs case we consider two different sets of values of (T_L, T_R) as indicated in Figure.

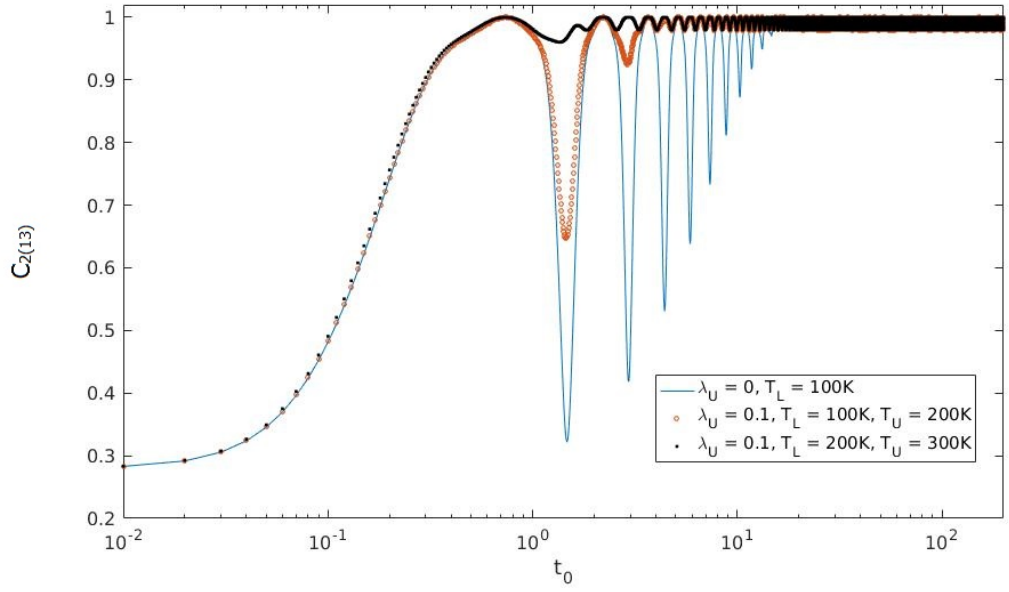

Figure 3.31: The concurrence $C_{2(13)}$ as a function of the scaling time t_0 for $p_1 = 0.3$, $p_2 = 0.5$, $p_3 = 0.5$ and fixed reservoir coupling parameter $\lambda_L = 0.1$ for a single reservoir as well as for double reservoirs. $\lambda_U = 0$ indicates the system of single reservoir, and $\lambda_U = 0.1$ indicates the system of double reservoirs. Here we consider the temperature of the single reservoir system, T_L, is 100K, and the temperature difference of the double reservoir system, $T_L \sim T_R$, is 100K. For double reservoirs case we consider two different sets of values of (T_L, T_R) as indicated in Figure.

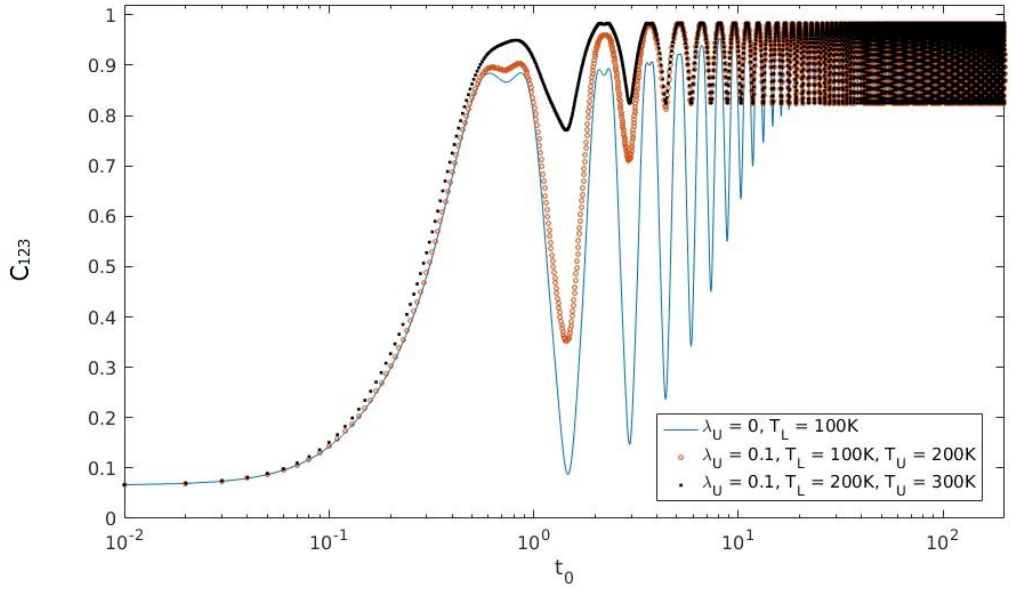

Figure 3.32: The concurrence C_{123} as a function of the scaling time t_0 for $p_1 = 0.3$, $p_2 = 0.5$, $p_3 = 0.5$ and fixed reservoir coupling parameter $\lambda_L = 0.1$ for a single reservoir as well as for double reservoirs. $\lambda_U = 0$ indicates the system of single reservoir, and $\lambda_U = 0.1$ indicates the system of double reservoirs. Here we consider the temperature of the single reservoir system, T_L, is 100K, and the temperature difference of the double reservoir system, $T_L \sim T_R$, is 100K. For double reservoirs case we consider two different sets of values of (T_L, T_R) as indicated in Figure.

4. Conclusion

In this thesis we analyze the dynamics of a spin chain consisting of three interacting spins (qubits), coupled to zero, one or two thermal reservoirs. The direct spin-spin interaction is given by the ubiquitous Heisenberg XX interaction Hamiltonian. We use the reduced density matrix approach to calculate the time evolution of the density matrices of various subsystems: single spins, pairs and the whole triple, by tracing out the remaining degrees of freedom (spins and reservoir). We study

- The populations of the spins (excitation probabilities), *i.e.*, the diagonal density matrix elements (energy basis).
- The entanglement (quantum correlations, measured by the concurrence) between spins, induced by their direct interaction and by the contact with their surroundings (thermal baths).

The main results we find are as follows.

- **Populations.** The dynamics of the populations is *periodic in time* and depends on the initial state of the spin chain. Since we consider energy-conserving interactions, the bath(s) do *not* influence the evolution of the populations at all. Nevertheless, they do change *coherences* (off-diagonal density matrix elements) and hence the quantum correlation (entanglement) between the spins.
- **Entanglement.** In the absence of interaction to the bath(s), the entanglement between spins oscillates in time. The amplitude of the entanglement oscillations depends on the initial state (some initial states will never get entangled (ferromagnetic states) while others reach almost maximal possible entanglement). As the interaction with the bath(s) is turned on, the entanglement evolves in a complicated way for initial, small times, but settles into a stationary (time oscillating) regime. The associated relaxation time depends on the bath temperatures and the system-bath coupling strength. The higher the coupling strength or the temperature, the quicker the stationary regime is reached.

4.1 Future Work

In applications to the problem of transfer of information in a quantum data bus, one would be interested in, say 10 qubits (spins), not just three. It would then be interesting to study an N qubit

chain coupled to heat baths and see how populations and correlations behave in time. (One might also study the case when N is very large, in case this facilitates the analytical part of the analysis). For the analytical part, one can use the reduced density matrix approach, as in the thesis here, or the Lindblad–Markovian master equation. For a fully numerical simulation we are thinking about quantum Monte Carlo simulations. It would also be interesting to relax the hypothesis of energy conserving interactions between spins and the baths. The resulting problem is much harder then, analytically, unless one is willing to assume some drastic simplifications (e.g., as mentioned above, an effective Markovian master equation approximation).

Bibliography

[1] A. Einstein, B. Podolsky, and N. Rosen, *Can Quantum-Mechanical Description of Physical Reality Be Considered Complete?*, Phys. Rev **47**, 777 (1935).

[2] E. Schrödinger, *Discussion of Probability Relations between Separated Systems*, Proc. Cambridge Philos. Soc. **31**, 555 (1935).

[3] S. Bose, *Quantum Communication through an Unmodulated Spin Chain*, Phys. Rev. Lett. **91**, 207901 (2003).

[4] M. Friesen, A. Biswas, X. Hu, and D. Lidar, *Efficient Multiqubit Entanglement via a Spin Bus*, Phys. Rev. Lett. **98**, 230503 (2007).

[5] S. Bose, *Quantum communication through spin chain dynamics: an introductory overview*, Contemp. Phys. **48**, 13 (2007).

[6] A. Kay, *A Review of Perfect State Transfer and its Application as a Constructive Tool*, Int. J. Quantum Inform. **08**, 641 (2010).

[7] S. Paganelli, S. Lorenzo, T. J. G. Apollaro, F. Plastina, and G. L. Giorgi, *Routing quantum information in spin chains*, Phys. Rev. A **87**, 062309 (2013).

[8] S. Lorenzo, T. J. G. Apollaro, A. Sindona, and F. Plastina, *Quantum-state transfer via resonant tunneling through local-field-induced barriers*, Phys. Rev. A **87**, 042313 (2013).

[9] S. Lorenzo, T. J. G. Apollaro, S. Paganelli, G. M. Palma, and F. Plastina, *Transfer of arbitrary two-qubit states via a spin chain*, Phys. Rev. A **91**, 042321 (2015).

[10] F. A. Mohiyaddin, R. Kalra, A. Laucht, R.Rahman, G. Klimeck, and A. Morello, *Transport of spin qubits with donor chains under realistic experimental conditions*, Phys. Rev. B **94**, 045314 (2016).

[11] R. R. Agundez, C. D. Hill, L. C. L. Hollenberg, S. Rogge, and M. Blaauboer, *Superadiabatic quantum state transfer in spin chains*, Phys. Rev. A **95**, 012317 (2017).

[12] M. C. Arnesen, S. Bose, and V. Vedral, *Natural Thermal and Magnetic Entanglement in the 1D Heisenberg Model*, Phys. Rev. Lett. **87**, 017901 (2001).

[13] Y. Sun, Y. Chen, and H. Chen, *Thermal entanglement in the two-qubit Heisenberg XY model under a nonuniform external magnetic field*, Phys. Rev. A **68**, 044301 (2003).

[14] M. Cao, and S. Zhu, *Thermal entanglement between alternate qubits of a four-qubit Heisenberg XX chain in a magnetic field*, Phys. Rev. A **71**, 034311 (2005).

[15] J. P. Cao, Z Z Sun, S Yin, Yupeng Wang, and X R Wang, *Magnetic impurity effect on the entanglement in the Ising model*, J. Phys. A **38**, 2579 (2005).

[16] V. Eisler, and Z. Zimboras, *Entanglement in the XX spin chain with an energy current*, Phys. Rev. A **71**, 042318 (2005).

[17] D. Burgarth, and V. Giovannetti, *Mediated homogenization*, Phys. Rev. A **76**, 062307 (2007).

[18] X. X. Zhang, and F. L. Li, *Generation of non-equilibrium thermal quantum discord and entanglement in a three-spin XX chain by multi-spin interaction and an external magnetic field*, Phys. Lett. A **375**, 4130 (2011).

[19] X. X. Yi, D. M. Tong, L. C. Kwek, and C. H. Oh, *Adiabatic approximation in open systems: an alternative approach*, J. Phys. B **40**, 281 (2007).

[20] O. V. Marchukov, A. G. Volosniev, M. Valiente, D. Petrosyan, and N. T. Zinner *Quantum spin transistor with a Heisenberg spin chain*, Nat. Commun. **7**, 13070 (2016).

[21] H.-P. Breuer, and F. Petruccione, *The Theory of Open Quantum Systems*, Oxford University Press, Oxford (2002).

[22] M. Merkli, G.P. Berman, and R. Sayre, *Electron Transfer Reactions: Generalized Spin-Boson Approach*, J. Math. Chem. **51**, Issue 3, 890 (2013).

[23] M. Merkli, G.P. Berman, A. Redondo, *Application of Resonance Perturbation Theory to Dynamics of Magnetization in Spin Systems Interacting with Local and Collective Bosonic Reservoirs*, J. Phys. A: Math. Theor. **44**, 305306 (2011).

[24] M. Merkli, G.P. Berman, H. Song, *Multiscale dynamics of open three-level quantum systems with two quasi-degenerate levels*, J. Phys. A: Math. Theor. **48**, 275304 (2015).

[25] M. Merkli, I.M. Sigal, G.P. Berman, *Dynamics of Collective Decoherence and Thermalization*, Ann. Phys. **323**, 373 (2008).

[26] M. Merkli, H. Song, *Overlapping Resonances in Open Quantum Systems*, Ann. Henri Poincaré **16**, Issue 6, 1397 (2014).

[27] M. Merkli, M. Mück, and I. M. Sigal, *Theory of Non-Equilibrium Stationary States as a Theory of Resonances*, Ann. Henri Poincaré **8**, Issue 4, 1539 (2007).

[28] D. B. Abraham, E. Baruch, G. Gallavotti, and A. Martin-Löf, *Dynamics of a local perturbation in the XY model. II-Excitations*, Studies in Appl. Math., 1:121, 1971.

[29] M. A. Nielsen and I. L. Chuang, *Quantum computation and quantum information*, Cambridge University Press, 2010.

[30] H. Araki and E.J. Woods, *Representations of the Canonical Commutation Relations Describing a Nonrelativistic Infinite Free Bose Gas*, J. Math. Phys. **4**, 637 (1963).

[31] M. Merkli, *Lecture Notes in Math*, **1880**,183 Springer, Berlin, 2006.

[32] O. Bratteli, D. Robinson, *Operator Algebras and Quantum Statistical Mechanics 1, 2*, Springer Verlag 2002.

[33] M. Christandl, N. Datta, A. Ekert, and A. J. Landahl, *Perfect State Transfer in Quantum Spin Networks*, Phys. Rev. Lett. **92**, 187902 (2004).

[34] M. Christandl, N. Datta, T. C. Dorlas, A. Ekert, A. Kay, and A. J. Landahl, *Perfect transfer of arbitrary states in quantum spin networks*, Phys. Rev. A **71**, 032312 (2005).

[35] J.Zhang, G. L. Long, W. Zhang, Z. Deng, W. Liu, and Z. Lu, *Simulation of Heisenberg XY interactions and realization of a perfect state transfer in spin chains using liquid nuclear magnetic resonance*, Phys. Rev. A **72**, 012331 (2005).

[36] D. Esteve, J.-M. Raimond, and J. Dalibard, *Lecture Notes of the Les Houches Summer School 2003*, Elsevier, 2004.

[37] W. K. Wootters, *Entanglement of Formation of an Arbitrary State of Two Qubits*, Phys. Rev. Lett. **80**, 2245 (1998).

[38] I. V. Proskuryakov, *Problems in Linear Algebra*, Mir Publishers, 1974, Problem 1082.

[39] P. Rungta, and C. M. Caves, *Concurrence-based entanglement measures for isotropic states*, Phys. Rev. A **67**, 012307 (2003).

[40] V. Coffman, J. Kundu, and W. K. Wootters, *Distributed entanglement*, Phys. Rev. A **61**, 052306 (2000).

[41] M. Merkli, G.P. Berman, F. Borgonovi, V.I. Tsifrinovich, *Creation of Two-Particle Entanglement in Open Macroscopic Quantum Systems*, Adv. Math. Phys., Article ID 375182, (2012).